Palaeontologia Electronica
palaeo-electronica.org

The long and icy journey of Mesozoic marine reptile vertebrae from northern Germany, their provenance and internal structures

Marco Schade, André Deutschmann, Christian Foth, Carina Paetzel, Tobias Püttmann, Michael Kenzler, and Sebastian Stumpf

ABSTRACT

Mesozoic vertebrate fossils within glacially transported deposits of Pleistocene age are rare. Here, we examine five isolated, strongly eroded vertebrae of Mesozoic marine reptiles, most probably plesiosaurs, from glacigenic sediments of northern Germany. In addition, three consecutive plesiosaur vertebrae, having already been described in previous publications, are briefly reconsidered. For one heavily eroded specimen, litho- and biostratigraphical analyses of associated sediment, including thin sectioning and calcareous nannofossil investigations, confirm a mid-Cretaceous age. The internal morphology of the five isolated vertebrae in focus, investigated with the help of microCT, reveals the presence of (neuro)vascular cavities within the respective centra. Unexpectedly, we found diverse internal cavity patterns which have only one feature in common: a medial pair of foramina on the floor of the neural canal that is connected to deep-reaching canals.

Marco Schade. University of Greifswald, Zoological Institute and Museum, Cytology and Evolutionary Biology, 17489 Greifswald, Germany. marco.schade@uni-greifswald.de
André Deutschmann. University of Greifswald, Institute of Geography and Geology, 17489 Greifswald, Germany. ad023399@uni-greifswald.de
Christian Foth. University of Fribourg, Department of Geosciences, 17000 Fribourg, Switzerland. christian.foth@gmx.net
Carina Paetzel. Western Norway University of Applied Sciences, Department of Civil Engineering and Environmental Sciences, 6856 Sogndal, Norway. carina.paetzel@hvl.no
Tobias Püttmann. Geological Survey of North Rhine-Westphalia, 47803 Krefeld, Germany. tobias.puettmann@gd.nrw.de
Michael Kenzler. University of Greifswald, Institute of Geography and Geology, 17489 Greifswald, Germany. kenzlerm@uni-greifswald.de
Sebastian Stumpf. University of Vienna, Faculty of Earth Sciences, Geography and Astronomy, Department of Palaeontology, 1090 Vienna, Austria. sebastian.stumpf@univie.ac.at

Final citation: Schade, Marco, Deutschmann, André, Foth, Christian, Paetzel, Carina, Püttmann, Tobias, Kenzler, Michael, and Stumpf, Sebastian. 2024. The long and icy journey of Mesozoic marine reptile vertebrae from northern Germany, their provenance and internal structures. Palaeontologia Electronica, 27(2):a33.
https://doi.org/10.26879/1313
palaeo-electronica.org/content/2024/5247-erratic-vertebrae

Keywords: Erratics, Mesozoic, marine reptiles, calcareous nannofossils, vertebrae, Germany

Submission: 22 June 2023. Acceptance: 28 May 2024.

INTRODUCTION

Before toothed whales and sharks took over the apex predator position in the oceans during the Cenozoic (or already in the Cretaceous in the case of certain shark genera like *Cretoxyrhina*; see Amalfitano et al. 2019), different groups of marine reptiles, such as ichthyosaurs, plesiosaurs, thalattosuchians and mosasaurs reigned the Mesozoic seas (e.g., Benson et al., 2012; Maxwell et al., 2012; Sachs et al., 2018). Whereas large parts of northern Germany are covered with relatively young glacigenic sediments of the Pleistocene, it belongs to the nature of such deposits that they occasionally contain re-deposited rock fragments and fossils from older Baltic-Scandinavian formations (see Foth et al., 2001; Sachs et al., 2016a; Sachs and Hornung, 2020, and references therein). Here, we report on three so far undescribed isolated vertebrae (GG 501, GG 502, UHKD500005) most likely belonging to plesiosaurs. In addition, we provide new anatomical information of two isolated (GG 422/2, GG 422/3) and three consecutive plesiosaur vertebrae (GPIH, unregistered), which have already been described in previous publications. All specimens come from different glacially influenced bed load localities in northern Germany. Plesiosaurs represent a group of marine reptiles that probably originated in the Late Triassic and thrived throughout the Mesozoic, reaching a worldwide distribution and considerable diversity (e.g., Benson et al., 2012; Fischer et al., 2017; Wintrich et al., 2017). All vertebrae of this study were discovered within the maximum Weichselian extent of the Scandinavian Ice Sheet (SIS; Hughes et al., 2016). To report and document these Mesozoic vertebrate remains, rarely found as erratics, and to get a better idea of their spatiotemporal and anatomical affinities, we conducted detailed morphological analyses; combined with stratigraphical age determination for one of the specimens.

Institutional Abbreviations

GD NRW, Geological Survey of North Rhine-Westphalia (Krefeld);
GG, Greifswalder Geologische Sammlungen, University of Greifswald;
GPIH, Institute for Geology, University of Hamburg;
LUNG-MV, State Agency for Environment, Nature Conservation and Geology of Mecklenburg Western-Pomerania (Güstrow);
SMNS, Staatliches Museum für Naturkunde, Stuttgart;
UHKD, Urzeithof Stolpe, Museumsstiftung.

MATERIAL AND METHODS

Generally, the platycoelous vertebrae in focus are strongly eroded and reveal cancellous bony tissue. The neural arch and transverse processes are usually broken off or completely missing if not mentioned otherwise.

GG 422/2 and 422/3

Whereas the specimen GG 422/2 represents a damaged cervical vertebra, GG 422/3 is a largely intact caudal centrum without the neural arch (described in Stumpf, 2016). In GG 422/2, large parts of the right lateral aspect of the centrum and neural arch are missing; the neural canal is still filled with sedimentary matrix. Both come from early Toarcian deposits near Grimmen in northeastern Germany that were glacially dislocated (Stumpf, 2016; Stumpf and Kriwet, 2019; Schade and Ansorge, 2022, and references therein); GG 422/3 was donated to the Greifswalder Geologische Sammlungen by Jens Kopka. As the outer morphology of both specimens has already been described in Stumpf (2016), we focus on their internal features revealed by microCT data.

GG 501

GG 501 was forwarded in 2020 to the Greifswalder Geologische Sammlungen by Steffen Ploetz, who found this fossil in a gravel pit near Wismar in the same year (Figure 1). This gravel pit is in the Weichselian sandur area of the post-LGM (Last Glacial Maximum) Pomeranian ice advance (LUNG 2010).

GG 502

GG 502 was forwarded to the Greifswalder Geologische Sammlungen by Gudrun Stollberg in 2012, who found this fossil on a beach section near Binz, island of Rügen (Figure 1). A secondary embedding in Pleistocene deposits, such as tills or other glacigenic material outcropping at the nearby

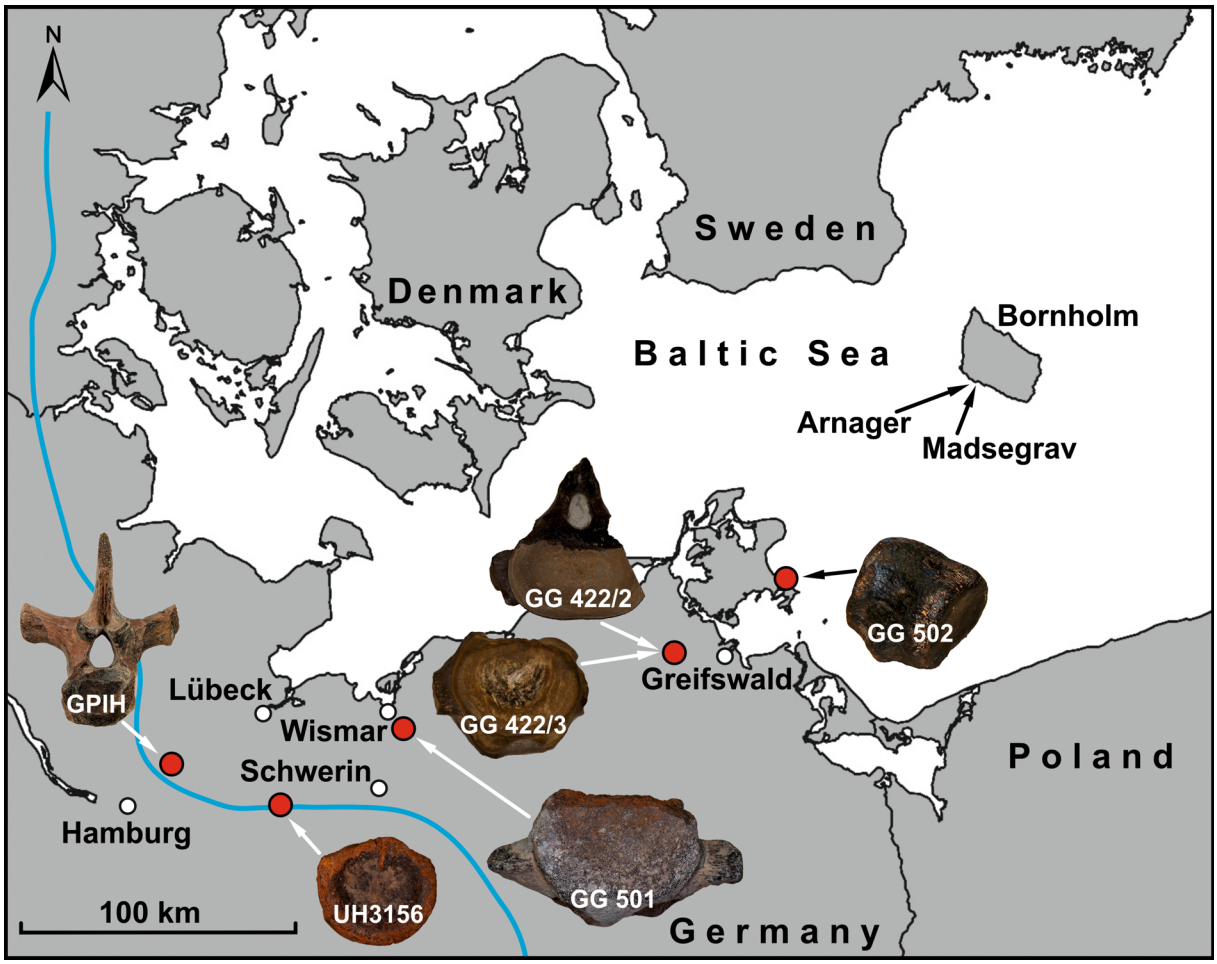

FIGURE 1. Map of the SW Baltic Sea area displaying the finding locations of the individual vertebrae. Note the indicated cliff outcrops of Lower Cretaceous deposits at Arnager and Madsegrav on Bornholm (Denmark). Blue line indicates maximal Weichselian ice extent.

cliff sections, is likely. However, as it was found isolated on the beach, an assignment to this sediment is not possible. Therefore, a correlation to a specific ice advance that carried along the vertebra to the site and a corresponding way of transport cannot be reconstructed.

UHKD500005

UHKD500005 (formerly UH3156) was lent to the Urzeithof Stolpe in 2022 by Stefan Polkowsky, who found this fossil in a gravel pit halfway between Hamburg and Schwerin in 2002 (Segrahner Berg; Figure 1).

GPIH, Unregistered

GPIH, unregistered (Institute for Geology, University of Hamburg) comprises three consecutive dorsal vertebrae with largely intact centra and neural arches. The vertebrae, first figured by Lehmann (1971) and Lierl (1990), have been briefly described by Sachs et al. (2016) based on archive images. The latter authors considered the vertebrae to come from a gravel pit near Hamburg and inferred an early Toarcian age.

MicroCT Imaging and Photogrammetry

The specimens GG 501 (voltage: 160 kV, X-ray tube current: 370 µA, exposure time: 3 s, voxel size: 0.065 mm) and GG 422/2 (voltage: 160 kV, X-ray tube current: 320 µA, exposure time: 3 s, voxel size: 0.043 mm) were scanned with a Viscom X8060 using a Viscom XT9190-THP transmission electron ray tube in the Vienna Micro-CT Lab (University of Vienna). GG 502 (voltage: 90 kV, X-ray tube current: 88 µA, exposure time: 20 s, voxel size: 0.04651 mm) and UHKD500005 (voltage: 90 kV, X-ray tube current: 88 µA, exposure time: 5 s, voxel size: 0.04641 mm) were scanned using the MicroXCT-200 device housed in the Zoological Institute and Museum, University of Greifswald,

whereas the specimen GG 422/3 (voltage: 130 kV, X-ray tube current: 61 µA, exposure time: 1,25 s, voxel size: 0.027 mm) was scanned with a Sky-Scan1173 in the Palaeontological Institute, University of Vienna. Digital segmentation was carried out using Amira (5.4.1), based on tiff image files. The microCT data were manually segmented to create 3D models of the internal cavities of GG 422/2, GG 422/3, GG 501, GG 502 and UHKD500005. The photogrammetry models are based on 369 (GG 501), 196 (GG 502) and 337 (UHKD500005) photographs and were created with Agisoft (1.3.4). The microCT slice data, segmented models (GG 422/2, GG 422/3, GG 501, GG 502 and UHKD500005) and photogrammetry models (GG 501, 502 and UHKD500005) are published online, on MorphoSource (Project: erratic vertebrae of Mesozoic marine reptiles from northern Germany - Schade et al. 2022 // MorphoSource). Additionally, the Greifswalder Geologische Sammlungen houses a 3D print of UHKD500005.

Petrography

GG 501 is poorly preserved, remarkably wide mediolaterally and displays long lateral processes on its mid-height. The latter feature seems rather unusual for plesiosaurs (see below) and on this basis, a cetacean identity cannot be excluded, since some taxa can show wide centra and prominent transverse processes on the mid-height of lumbar and caudal vertebrae (e.g., Bianucci et al., 2018). Hence, it was important to classify GG 501 stratigraphically to exclude a much younger cetacean owner. A provenance analysis was performed based on sediment associated with GG 501, however, the other vertebrae could not be sampled due to the lack of sufficient amounts of accessible sediment. Firstly, sediment of GG 501 was extracted with a pneumatic graver and subsequently embedded in epoxy resin before being processed to a thin section (GG 501-TS), following the standard procedure given by MacKenzie et al. (2017). For comparison, a subsample of the outcrop sample (MV400005, part of the national collection of LUNG-MV) from the base of the Cenomanian Arnager Greensand Formation (cliff of Madsegrav east of Arnager, island of Bornholm, Denmark; Figure 1) was prepared for thin section analysis as well (MV400005-TS). An Epson Perfection V850Pro flatbed scanner (De Keyser 1999), belonging to the equipment of the Institute of Geography and Geology, produced high-resolution images of 2400 dpi for both thin sections (GG 501-TS, MV400005-TS). The petrographic analysis was carried out with a Zeiss Axioskop polarization microscope, equipped with an AxioCam HRc, housed in the Institute of Geography and Geology as well.

Calcareous Nannofossils

For age determination of GG 501, a sediment subsample from the matrix was investigated at the GD NRW for calcareous nannofossils. Two simple smear slides (GG 501-N1, GG 501-N2) were prepared from the glauconitic, calcareous sandstone, following the preparation technique by Perch-Nielsen (1985). Additionally, two smear slides (MV400005-N1, MV400005-N2) were prepared from the MV400005 reference sample. This reference sample was collected from the Arnager Greensand Formation of Bornholm (Denmark), which was suspected to represent a probable source rock.

At least five traverses of medium particle density were screened under a Leica DM2700P cross-polarized light microscope at a magnification of 1500x (housed in the GD NRW in Krefeld). Calcareous nannofossil biostratigraphy is based on first and last occurrences (FOs, LOs) of index taxa, following the BC- and UC-zonation schemes (BC = Boreal Cretaceous, UC = Upper Cretaceous) of Bown et al. (1998) and Burnett (1998). All nannofossil samples (GG 501-N1, GG 501-N2, MV400005-N1, MV400005-N2) are stored at the GD NRW.

RESULTS AND DISCUSSION

Description of GG 501

Plesiosauria gen. et sp. indet.?
Figure 2

The centrum is partly covered in greenish glauconitic sandstone (Figure 2). Additionally, its surface is strongly eroded, revealing cancellous bony tissue. Both articular facets are around 8 cm in mediolateral width. The preserved part of the anterior articular facet is 6 cm in dorsoventral height, while the posterior one is 5.5 cm high. The anterior articular facet is mostly covered by sediment. However, it is still conceivable that both articular facets are slightly concave and oval-shaped, being wider than high. The centrum is 4.5 cm in anteroposterior length and on its mid-length about as wide as the articular facets. One side of the centrum, which is herein interpreted as the dorsal one, is rather straight, while the antagonistic ventral side is rather convex. The dorsal side of the centrum is largely eroded, showing two subcircular foramina

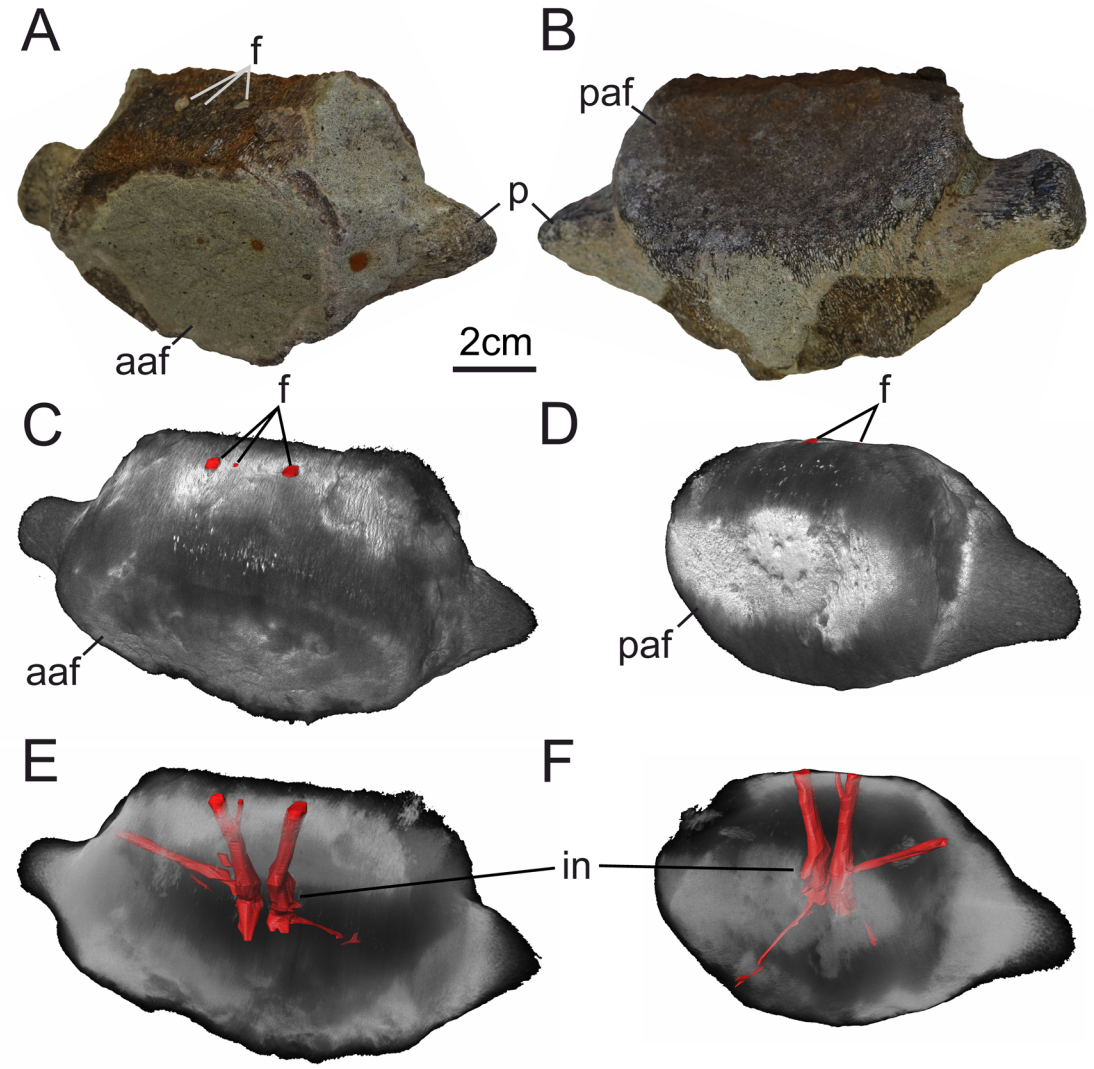

FIGURE 2. GG 501, photographs **A, B** of (?anterior pectoral) vertebral centrum in **A** anterodorsolateral and **B** posteroventrolateral view. CT renderings **C-F** of GG 501 in **C, E** anterodorsolateral view and **D, F** posterolateral view. Abbreviations: aaf, anterior articular facet; f, foramen; in, internal network; p, process; paf, posterior articular facet.

of 0.5 cm width. The foramina are medially positioned, separated from each other by a space of 1.2 cm. The surface of the ventral side is eroded and covered by sediment in different aspects. The bases of two processes are preserved and situated on the mid-height and mid-length of the centrum. Both processes are slightly inclined posteriorly, but project mainly laterally. The remnants of the processes are 2.5 cm in mediolateral length and dorsoventrally as high on their bases.

The microCT data of GG 501 show that there are three foramina on the floor of the neural canal, the medial one of which leads to a short canal that merges with the right canal (Figure 2C, E, F). The two main canals reach deep into the centrum, where they seem to stay separate from each other. Close to the core of the centrum, the right canal is connected to another, smaller canal that is dorsolateral oriented and should have a respective foramen posterodorsally to the right process, in an area that is still covered in sedimentary matrix. Ventrally, again in the vicinity of the core, both canals that bear dorsal foramina, communicate with a thin lateroventral and slightly posterior leading canal each. Because of the solution of the microCT data, it was not possible to fully reconstruct the right one, however, the left one was traceable and could have had a foramen close to

the edge between the posterior articular facet and the ventral surface of the centrum; this area is eroded and partly covered with sedimentary matrix.

Petrography of GG 501

Subsample GG 501-TS. Based on macro- and microscopic investigations of the host sediment, the vertebra was originally embedded in a glauconite-rich calcitic cemented sandstone. At least 50-60% of the investigated thin section is composed of fine-grained sand, which is subrounded to rounded. The cement consists of carbonate and accounts for 20-30% of the thin section. It is characterised by a relatively high proportion of sandy, dark green to brownish green glauconite (15-20%), while the content of feldspar is less than 5%. In addition, isolated opaque phosphate nodules with an average size of about 100 µm are present, as well as rare occurrences of foraminifera remains and indetermined spherical bioclasts (Figure 3).

Subsample MV400005-TS. The composition of the outcrop sample MV400005-TS from the base of the Cenomanian Arnager Greensand Formation consists of 50-60% angular to subrounded quartz grains, displaying a bimodal distribution of the grain size in the fraction ~70 µm and ~600 µm (Figure 4). Greenish glauconite grains occur scattered and account for 10-15% of the total amount of grains. The grain size of the glauconite ranges between coarse-grained silt to medium-grained sand, whereby the larger fraction tending to be better rounded. At least 5% of the thin section is composed of opaque phosphate nodules with a dominant grain size of 100-200 µm (Figure 4). The calcitic cement accounts for 20-25% of the sample.

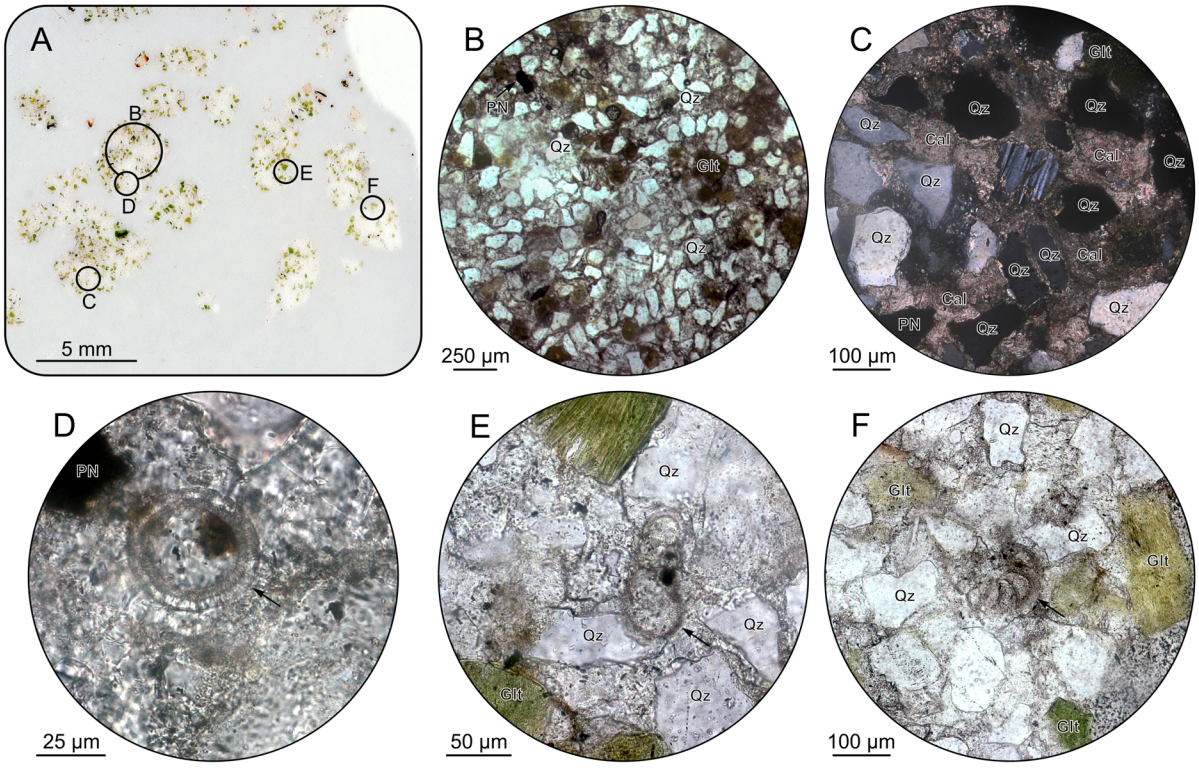

FIGURE 3. Overview scan of thin section GG 501-TS **A** with microscopical close-up photos of various domains of the extracted and processed cuttings. Representative microscopic views of the sediment composition, under **B** plane-polarized light (ppl) and under **C** crossed polarized light (xpl), showing the high amounts of subrounded quartz (Qz), glauconite (Glt) and the calcitic cement (Cal). Note the dispersed phosphate nodules (PN) at the bottom left. **D** Unspecified calcitic spheroidal microfossil (black arrow) next to a phosphate nodule (ppl). **E** Peripheral view of a chambered calcareous foraminifera (black arrow), possibly resembling a *Muricohedbergella portsdownensis* (Williams-Mitchell, 1948) from the Cenomanian surrounded by quartz and glauconite grains (ppl). **F** Unspecified fragment of a chambered calcareous foraminifera fossil (black arrow). Note the glauconite (Glt) sand-sized grains in typical greenish and greenish-brown color at plane polarized light.

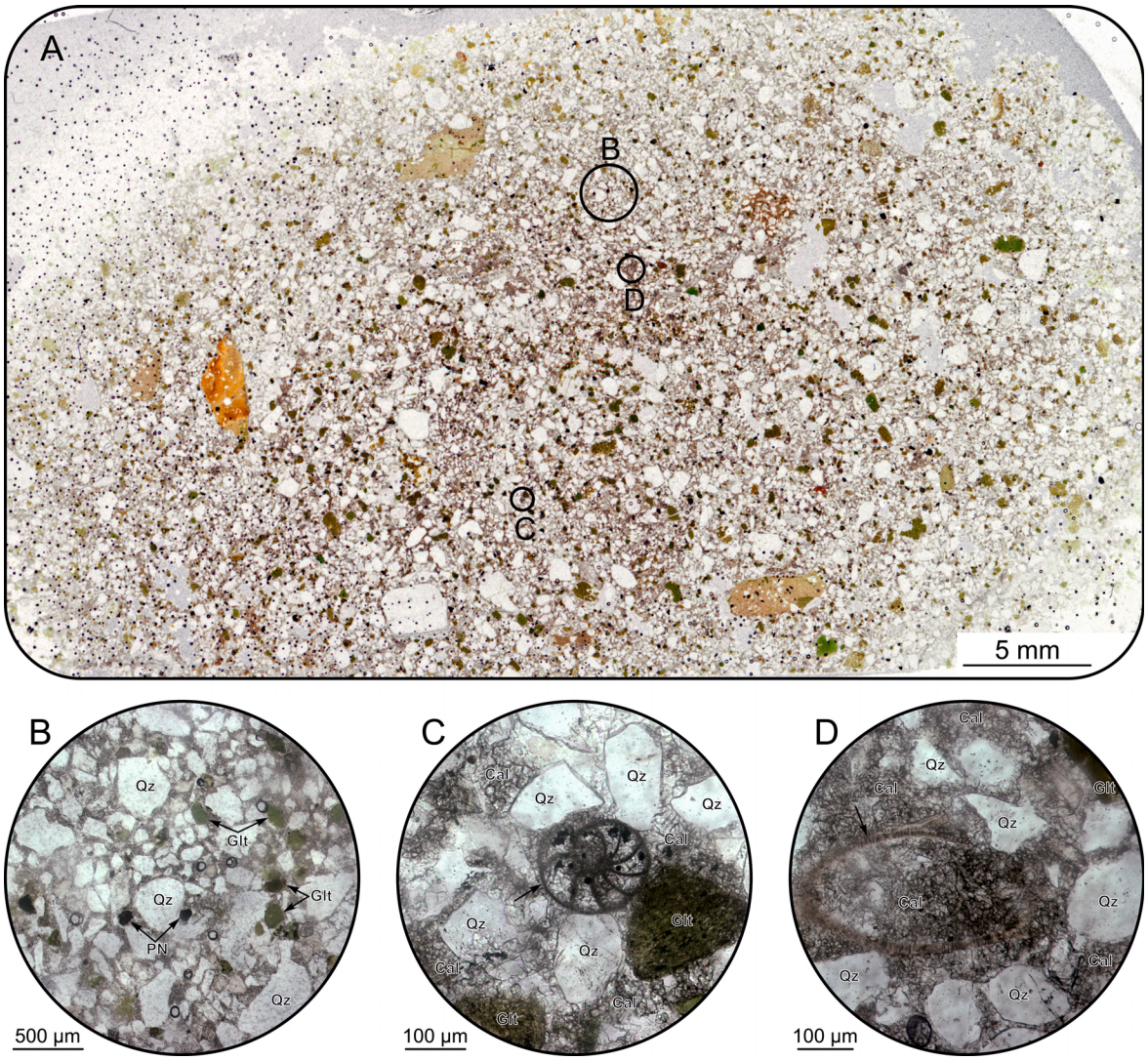

FIGURE 4. Overview scan of thin section MV400005-TS **A** displaying a domination of quartz and glauconite grains within calcitic cement. Note several lithoclasts indicated, which exhibit a reddish and brownish matrix, quartz grains, and dispersed glauconite. The evenly distributed glauconite (Glt) appear in typical green and brownish color. **B** Subrounded sand-sized quartz grains (Qz) and smaller subangular quartz grains dominate the thin section, whereas glauconite (Glt) and phosphate nodules (PN) occur dispersed. **C** A lateral view of a chambered calcareous foraminifera fossil (black arrow) located within the calcitic cement sourrounded by quartz (Qz) and glauconite (Glt) grains. **D** Bioclast, most likely a mollusc of unknown identity (black arrow). Note that all microscopic views were taken under plane polarized light.

Lithological Comparison of Sample GG 501 and Sample MV400005

An initial macroscopic examination of the adherent sediment of sample GG 501 revealed a lithologic composition of quartz, phosphorite nodules, glauconite grains, and calcitic cement. Considering that the specimen was transported by the SIS to the place where it was found, only the bottom of the Baltic Sea, the area of southern Sweden and the island of Bornholm, can be assumed as delivery areas. Since the vertebra was found as an isolated specimen, a relatively short transport route can be assumed; otherwise, the specimen would have been completely worn down. The character of the attached sediment, especially the presence of phosphate aggregates suggests a very slow rate of deposition during sedimentation. Comparable sedimentary features are known from the basal Cenomanian as they are outcropping on Bornholm (Graversen, 2004; Elicki and Magnus, 2012). In addition, isolated outcrops of Paleogene phosphorite deposits are known from the southern Bal-

tic Sea area (Kharin, 2009). However, further occurrences of glauconite-bearing sediments in the catchment area of the SIS are found in early Cambrian sandstones, Ordovician limestones, calcareous marlstones, dolomites, dolomitic marlstones, Cretaceous sandstones and limestones, and middle Miocene sandstones (Shogenova et al., 2003). Nevertheless, direct lithological comparison of the samples (GG 501 and MV400005) reveals many similarities. Differences are found only marginally in the degree of grain rounding, and individual components vary only slightly in their percentual occurrence. In the area of the outcrop at Arnager and Madsegrav, two banks containing phosphorite concretions are exposed: one at the base of the Arnager Greensand (early Cenomanian) and one at the base of the Arnager Limestone (early Coniacian). The comparison sample MV400005 is from the basal part of the Arnager Greensand and shows many similarities to the sample GG 501 regarding petrography. Thus, the vertebra may be regarded as early Cenomanian, although a minimum age of early Coniacian cannot be excluded on a lithological basis.

Calcareous Nannofossils of GG 501

All nannofossil subsamples (GG 501-N1, GG 501-N2, MV400005-N1, MV400005-N2) contain nannofossil assemblages of only moderate to poor preservation. Nannofossil abundances are relatively low, with *Watznaueria barnesiae* being the dominating species in all samples. A total of 34 and 30 different nannofossil taxa is identified in the GG 501-N1 and GG 501-N2 subsamples, respectively. In the MV400005-N1 and MV400005-N2 subsamples, the species richness is only 14 and 22. Selected calcareous nannofossils are illustrated in Figures 5 and 6. All nannofossil taxa identified in the samples are indicated in Table 1 and the Taxonomic Index.

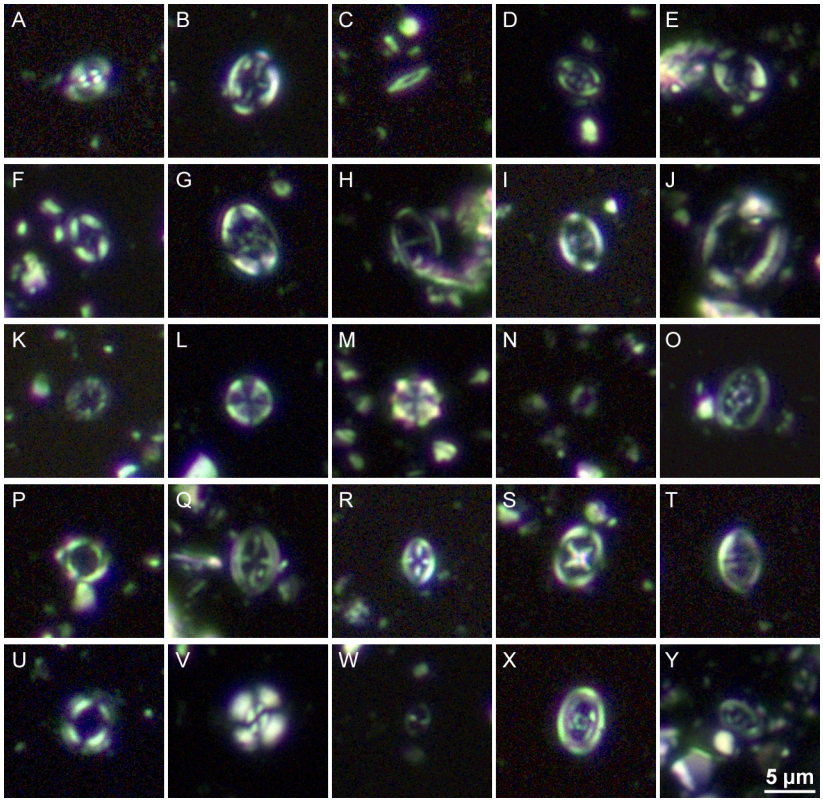

FIGURE 5. Selected calcareous nannofossils from the samples GG 501-N1 and G 501-N2 (cross-polarized light) in alphabetical order. **A** *Biscutum constans*; **B** *Broinsonia matalosa*; **C** *Calciosolenia fossilis*; **D** *Eiffellithus equibiramus*; **E** *Eiffellithus monechiae*; **F** *Eiffellithus paragogus*; **G** *Eiffellithus turriseiffelii*; **H** *Gartnerago theta*; **I** *Gorkaea operio*; **J** *Manivitella pemmatoidea*; **K** *Prediscosphaera columnata*; **L** *Radiolithus planus*; **M** *Radiolithus undosus*; **N** *Repagulum parvidentatum*; **O** *Rhagodiscus hamptonii*; **P** *Rotelapillus crenulatus*; **Q** *Staurolithites gausorhethium*; **R** *Staurolithites laffittei*; **S** *Tegumentum stradneri*; **T** *Tranolithus orionatus*; **U** *Tubirhabdus burnettiae*; **V** *Watznaueria barnesiae*; **W** *Zeugrhabdotus erectus*; **X** *Zeugrhabdotus howei*; **Y** *Zeugrhabdotus xenotus*. Scale bar valid for all specimens.

Biostratigraphy

The identified index taxa from GG 501 include *Eiffellithus turriseiffelii* (FO at the base of BC27a/UC0, late Albian; Figure 5G) and *Zeugrhabdotus xenotus* (LO defines the top of the biozone UC2a, early Cenomanian; Figure 5Y). Thus, the host rock of GG 501 is of late Albian to early Cenomanian age (UC0–UC2a). Additionally, the species *Gorkaea operio* (Figure 5I), *Rhagodiscus hamptonii* (Figure 5O) and *Tubodiscus burnettiae* (Figure 5U) are documented by single specimens only. These taxa are restricted to Albian strata (Bown, 2001; Watkins and Bergen, 2003).

The taxa identified in samples MV400005-N1 and MV400005-N2 include *Eiffellithus turriseifelii* (Figure 6D-E) and *Gartnerago theta* (LO defines the top of the biozone UC3a, early mid-Cenomanian; Figure 6G). Thus, the sample MV400005 is of late Albian to early mid-Cenomanian age. A single, uncertain specimen of *Lithraphidites* cf. *acutus* (FO defines the base of biozone UC3a; Figure 6I) points to an early mid-Cenomanian age. Unfortunately, this refinement could not be verified by the observation of a more indicative specimen of *L. acutus* in this sample. In addition to the absence of taxa typical for Albian and lowermost Cenomanian strata, the sample is of early to early mid-Cenomanian age and likely correlates to the upper part of the Arnager Greensand Formation (Figure 7).

Stratigraphic Implications for GG 501

Based on the combined litho- and biostratigraphical observations, the sediment in which the vertebra GG 501 was embedded can be classified into the late Albian to early Cenomanian. Due to potential reworking of Albian macro- and microfossils as suggested by earlier studies (Schiøler, 1992; Hart et al., 2012), the nannofossil assemblages can be assigned to the lower part of the Arnager Greensand Formation. This correlation is supported by the presence of phosphate nodules, Figures 3, 7).

Description of GG 502

Plesiosauria gen. et sp. indet.?
Figure 8

Due to the preservation of the specimen, it is not possible to securely identify the anterior or posterior side of the centrum. The centrum is characterized by a high density; a brownish coloration of the surface indicates the presence of hematite.

The dorsal and ventral sides of the centrum are both 5 cm in length and width, as preserved. Both slightly concave articular facets suggest an almost heart-shaped morphology, being mediolaterally narrower ventrally than dorsally. Both articular facets are about 4.5 cm in mediolateral width and 4 cm in dorsoventral height. On its dorsal side, the floor of the neural canal is still perceivable as a medially positioned and anteroposteriorly oriented depression. With the aid of our microCT data, two

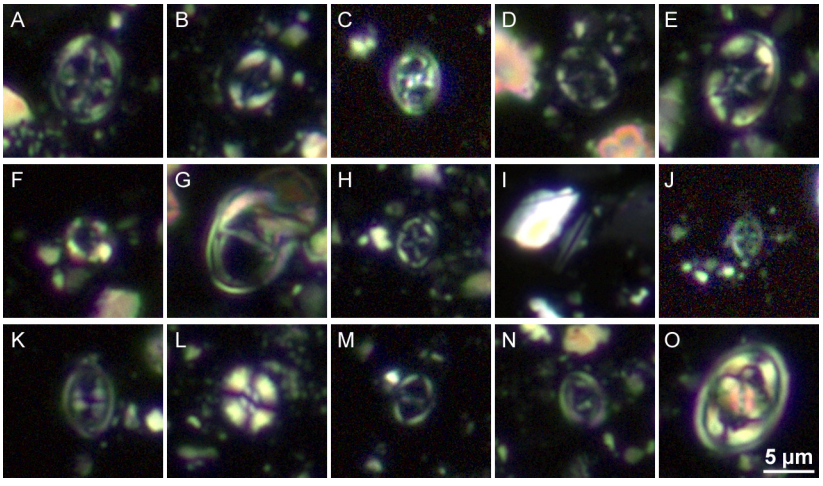

FIGURE 6. Selected calcareous nannofossils from the sample MV40005-N2 (cross-polarized light) in alphabetical order. **A** *Axopodorhabdus albianus*; **B** *Broinsonia signata*; **C** *Chiastozygus litterarius*; **D**, **E** *Eiffellithus turriseiffelii*; **F** *Eprolithus apertior*; **G** *Gartnerago theta*; **H** *Helicolithus compactus*; **I** *Lithraphidites* cf. *acutus*; **J** *Staurolithites laffittei*; **K** *Tranolithus orionatus*; **L** *Watznaueria barnesiae*; **M** *Zeugrhabdotus acanthus*; **N** *Zeugrhabdotus bicrescenticus*; **O** *Zeugrhabdotus embergeri*. Scale bar valid for all specimens.

TABLE 1. Calcareous nannofossil species determined in the samples GG 501-1 and MV400005. MP = moderate to poor, P = poor, VP = very poor preservation, L = low abundance. Biozones follow Burnett (1998). ● taxon present, ≥ 2 specimens. ○ taxon present, single specimen

Sample	GG 501-N1	GG 501-N2	MV400005-N1	MV400005-N2
Nannofossil preservation	MP	P	VP	P
Nannofossil abundance	L	L	L	L
Biozone	UC0-UC2a		UC0-UC3a	
Species richness (SR)	34	30	14	22
Axopodorhabdus albianus				●
Biscutum constans	●	●		●
Broinsonia matalosa	●		●	
Broinsonia signata		●	●	●
Bukrylithus ambiguus	○	●		
Calciosolenia fossilis	●	●		
Chiastozygus litterarius	●		○	●
Chiastozygus platyrhetus	○			○
Chiastozygus spissus	○			
Chiastozygus synquadriperforatus			●	
Cribrosphaerella ehrenbergii		●		
Cyclagelosphaera margerellii	○		●	●
Discorhabdus ignotus		●		
Eiffellithus equibiramus	●	●		
Eiffellithus monechiae		●		
Eiffellithus paragogus		●		
Eiffellithus turriseiffelii	●	●		●
Eprolithus apertior				●
Gartnerago theta	●	●	●	●
Gorkaea operio	○	○		
Helicolithus compactus		●		●
Litraphidites cf. acutus				○
Manivitella pemmatoidea		●		
Prediscosphaera columnata	●	●	●	
Prediscosphaera cretacea		●		
Radiolithus orbiculatus	●	●		
Radiolithus planus	○			
Radiolithus undosus	●			
Repagulum parvidentatum	●	●	○	
Retecapsa crenulata	○			
Rhagodiscus angustus		●		○
Rhagodiscus hamptonii	○			
Rhagodiscus splendens				●
Rotelapillus crenulatus		●		
Sollasites horticus	●	●		○
Staurolithites ellipticus	●		●	●
Staurolithites gausorhethium	●	●		
Staurolithites lafittei	●		●	●

Sample	GG 501-N1	GG 501-N2	MV400005-N1	MV400005-N2
Tegumentum stradneri		●		
Tranolithus orionatus	●	●	●	●
Tubodiscus burnettiae	○			
Watznaueria barnesiae	●	●	●	●
Watznaueria baticlypeata	○			
Zeugrhabdotus acanthus	●			●
Zeugrhabdotus bicrescenticus	●	●	●	●
Zeugrhabdotus diplogrammus	●	●		
Zeugrhabdotus embergeri				●
Zeugrhabdotus erectus	●	●		
Zeugrhabdotus howei	●	●		
Zeugrhabdotus trivectis	●	●	●	●
Zeugrhabdotus xenotus	●			

foramina are discernable, closely to one another (0.5 cm), on the floor of the former neural canal (Figure 8A). The neurocentral articular facet is strongly eroded, but still slightly elevated. In lateral view, the centrum is slightly medially constricted. The base of a process for rib articulation is still preserved, measuring 0.5 cm in mediolateral length. The process is positioned on the dorsal half of the centrum, close to the neurocentral articular facet. In lateral view, the process is positioned on the mid-length of the centrum and triangular in cross section. A circular foramen with a width and height of 0.3 cm is located on the ventral half of the centrum. The circular foramen is ventrally to the process. The other lateral side of the centrum bears such a foramen on a slightly higher position. One half of the ventral side of the centrum is strongly eroded, but together with the anterior and posterior articular facet morphology, the centrum gives the impression of having borne an anteroposteriorly oriented keel as ventralmost edge. Furthermore, as the microCT data suggest, three additional foramina are present on the ventral side of the centrum, close to or within the ventral eroded patch. Hence, the internal network within the centrum bears two foramina dorsally and five ventrolaterally to ventrally, resulting in a hand-like appearance (Figure 8B, C). The individual canals seem to have related to each other close to the core of the centrum. The whole network occupies only an anteroposteriorly narrow space and is not exactly situated on the anteroposterior mid-length of the centrum (Figure 8D).

Description of GG 422/2 and GG 422/3

Plesiosauroidea gen. et sp. indet.
Figures 9, 10, 11

As the external morphology of these two specimens has already been described by Stumpf (2016; GG 422/2 was interpreted to represent a posterior cervical, whereas GG 422/3 is a caudal centrum), we herein focus on their internal structures. The microCT data of GG 422/2 show the presence of two vertical canals directly below the floor of the neural canal, reaching about 1.3 cm deep (Figure 10B). The microCT data suggest that the core of the centrum bears no canal or cavity network, however, this could be due to the low-density contrast in this area. Four canals that are associated with respective foramina on the ventral surface could be reconstructed (Figure 10C, D). The more laterally positioned foramina reach some 1.3 cm deep dorsally, whereas the smaller medial foramina lead over to thinner and shorter canals.

The specimen GG 422/3 displays two dorsal foramina on the neural canal floor (Figure 11A, B). They are leading into the core of the centrum where they seem connected with each other. Furthermore, both canals are connected to one other canal on each side of the centrum that is lateroventrally oriented and opens into a foramen on the ventrolateral aspect. The left ventrolateral aspect of the centrum bears two foramina, one of which seemingly not reaching into the core of the centrum. Additionally, there are several small foramina on the ventral aspect of the centrum that seem not to lead over to deep canals (Figure 11C, D).

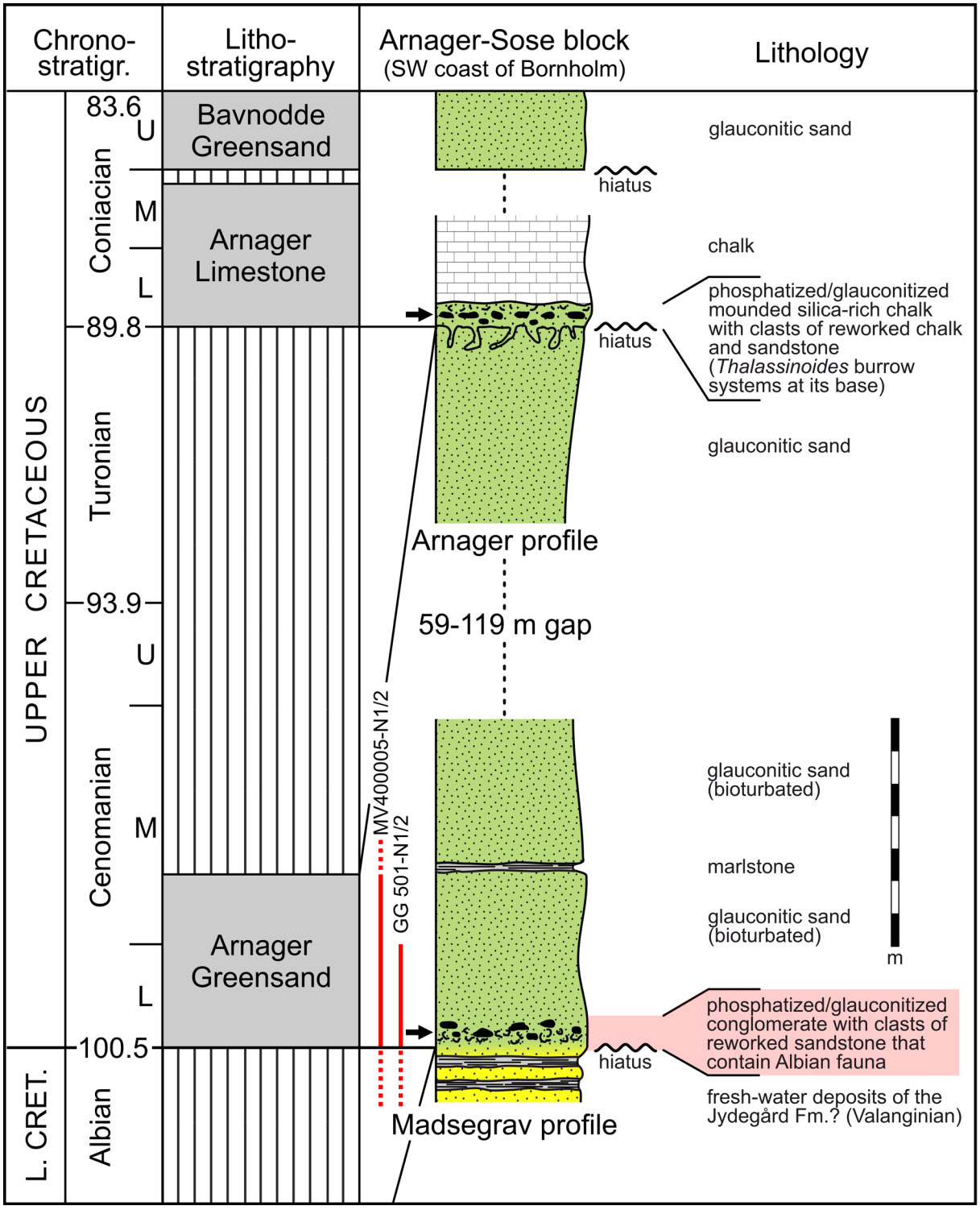

FIGURE 7. Stratigraphy of the outcropping strata at the Arnager and Madsegrav cliff section on the island of Bornholm (Denmark; see Figure 1). Based on the comparative provenance analysis of thin sections GG 501-TS and MV400005-TS, the sediment in which GG 501 was embedded, could be either part of the base of the Arnager Limestone or the base of the Arnager Greensand (black arrows). With the additional results of biostratigraphic interpretations of the outcrop sample MV400005 (nannofossils of MV400005-N1 and MV400005-N2) and the sample of adherent sediment of specimen GG 501 (nannofossils of GG 501-N1 and GG 501-N2), indicated by the red bars, an unambiguous stratigraphic classification of GG 501 to the Lower Cenomanian is established (shaded in red to the right; compiled and adapted from Hart, 1979; Hart et al., 2012; Cohen et al., 2013; Hajny, 2016; Svennevig and Surlyk, 2019).

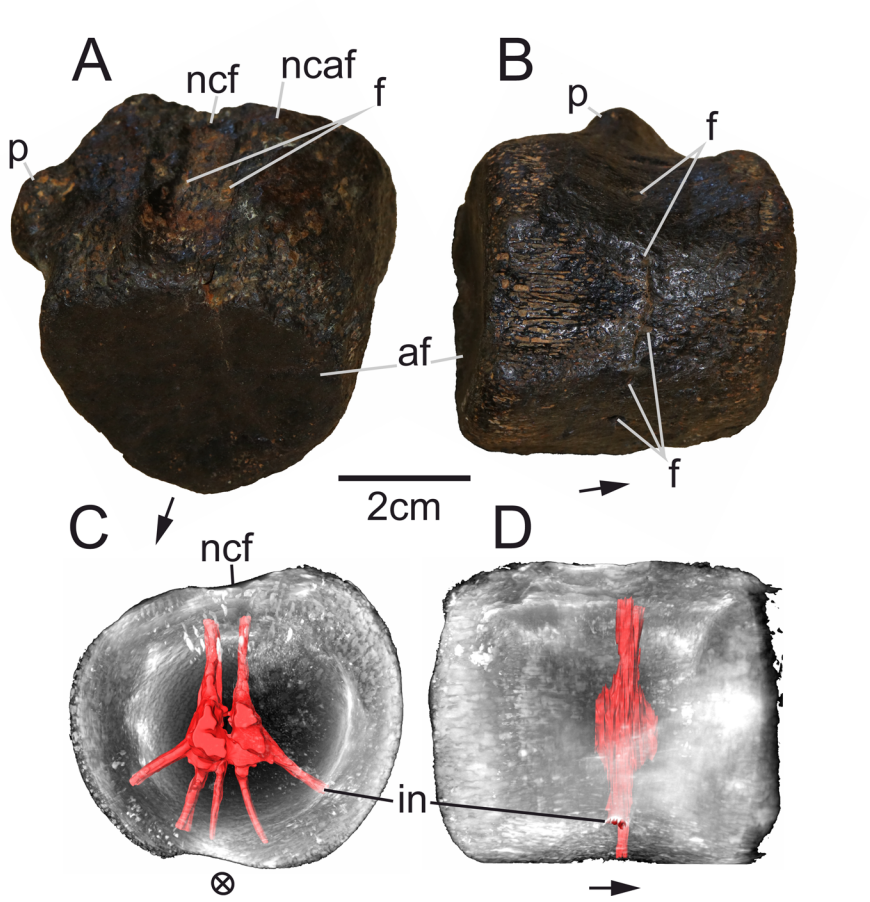

FIGURE 8. GG 502, photographs **A**, **B** of (?posterior pectoral) vertebral centrum in **A** antero/posterodorsal and **B** ventral view. CT renderings **C**, **D** of GG 502 in **C** anterior/posterior view and **D** lateral view. Abbreviations: af, articular facet; f, foramen; in, internal network; ncaf, neurocentral articular facet; ncf, floor of neural canal; p, process. Arrows point where the largely intact heart-shaped articular facet faces.

Description of UHKD500005

Plesiosauria gen. et sp. indet.?
Figures 12, 13

Because of its condition, it is not possible to securely identify the anterior or posterior side of the centrum. Additionally, the anterior or posterior articular facet is partly covered in greyish sediment, while a mixture of rounded sediment grains and blackish precipitates (probably containing pyrite) occur on one dorsolateral side of the centrum. Both articular facets are subcircular, measuring about 4 cm in mediolateral width and 3.5 cm in dorsoventral height. The centrum measures about 2.5 cm in anteroposterior length.

As the microCT data suggest, two foramina are present on the dorsal side of the centrum. One foramen is covered by a black sediment accumulation. The other one is close to the dorsalmost part of the centrum and barely discernable externally (Figure 12A, B).

The dorsal side of the centrum is dorsolaterally depressed. There seems to be a left and a right depression, separated from each other by an anteroposteriorly oriented median elevation. Furthermore, both depressions are separated from their respective lateral side of the centrum by one anteroposteriorly oriented and ventrally convex ridge each. In lateral view, the centrum is slightly medially constricted. Ventrally to each lateral ridge, one subcircular foramen is present on both sides. Both foramina are approximately 0.2 cm in width. Ventrally to both foramina are two slight depressions each. The microCT data show that only one of them seems not to penetrate the bone. On the ventral side of the centrum, one large and two smaller foramina are present. Thus, the internal network of the centrum bears two canals dorsally and three ventrally. Furthermore, three depres-

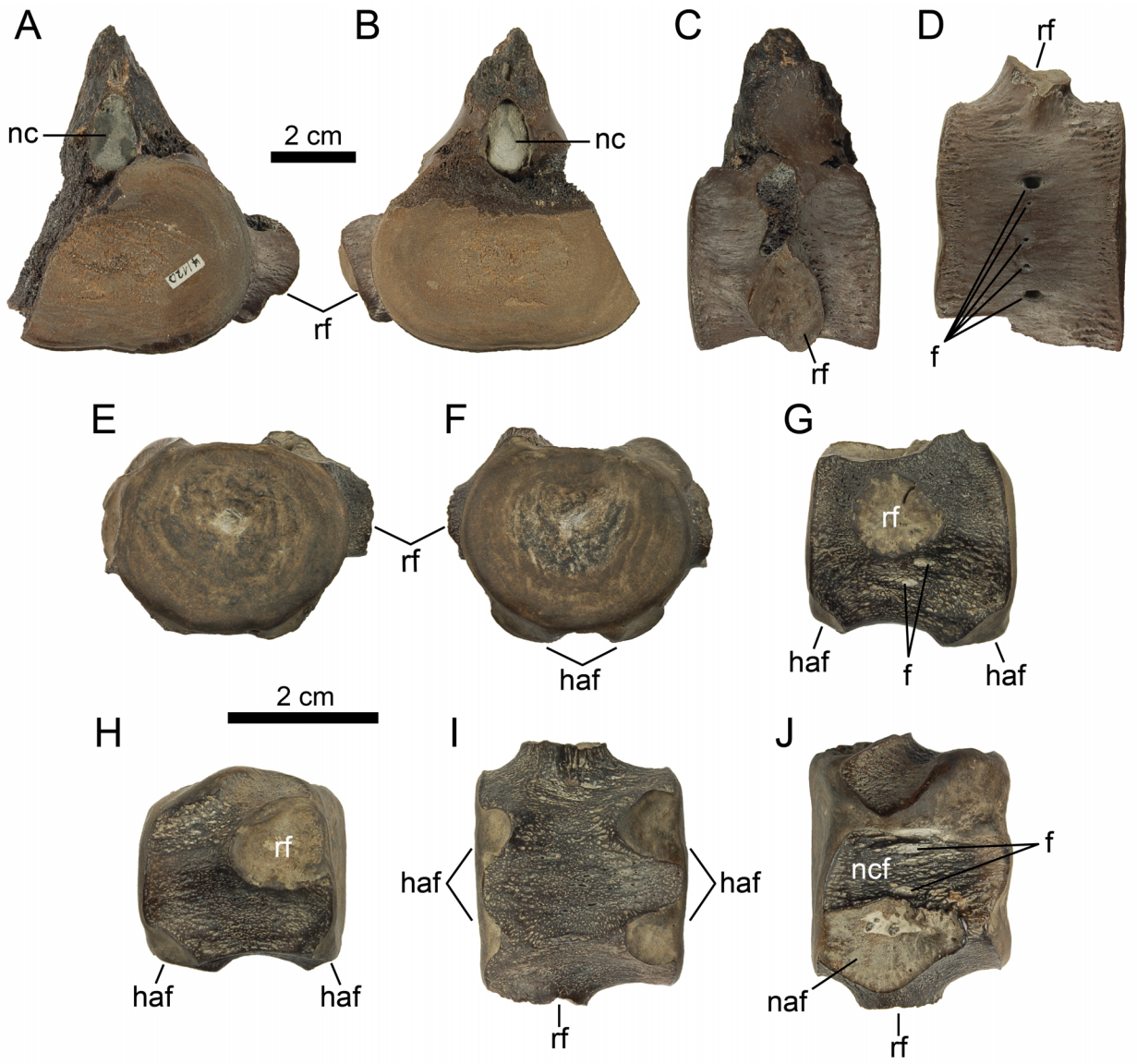

FIGURE 9. GG 422/2, a posterior cervical vertebra from the lower Toarcian of Grimmen (**A–D**) in **A** anterior, **B** posterior, **C** left lateral and **D** ventral view. GG 422/3, a caudal vertebral centrum from the lower Toarcian of Grimmen (**E–J**) in **E** anterior, **F** posterior, **G** left lateral, **H** right lateral, **I** ventral and **J** dorsal view. Abbreviations: f, foramen; haf, haemal arch facet; naf, neural arch facet; nc, neural canal; ncf, neural canal floor; rf, rib facet.

sions or foramina are present on each lateral side. However, on one lateral side, only two foramina penetrate the bone. While seven out of 10 canals are clearly traceable into the core of the centrum, three of them (ventrally and laterally) do not reach far internally or appear to be very superficial penetrations (Figure 12F, G). The microCT data suggest that this network mainly consists of canals, which may be connected via a distally diffuse cavity in the core of the centrum (Figures 12F; 13). The whole network occupies only an anteroposteriorly narrow space and is situated on the anteroposterior mid-length of the centrum (Figure 12C, G).

Description of GPIH, unregistered

Sauropterygia Owen, 1860
Plesiosauria de Blainville, 1835
Plesiosauroidea Welles, 1943
Microcleididae Benson, Evans and Druckenmiller, 2012
Figure 14

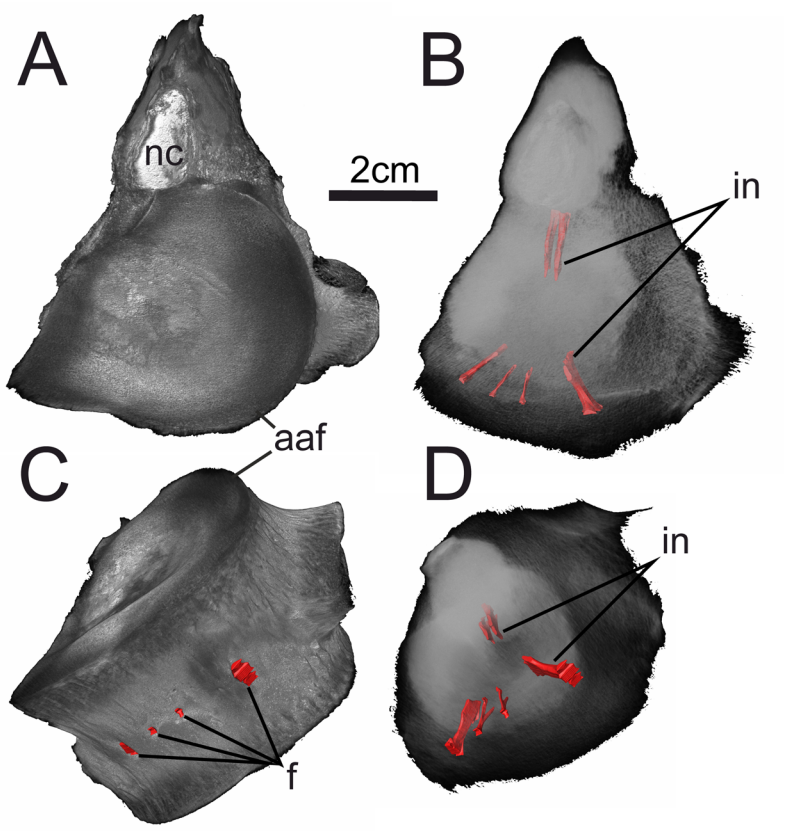

FIGURE 10. GG 422/2, CT renderings **A-D** of (posterior cervical) vertebra in **A, B** anterior and **C, D** anteroventrolateral view. Abbreviations: aaf, anterior articular facet; f, foramen; in, internal network; nc, neural canal.

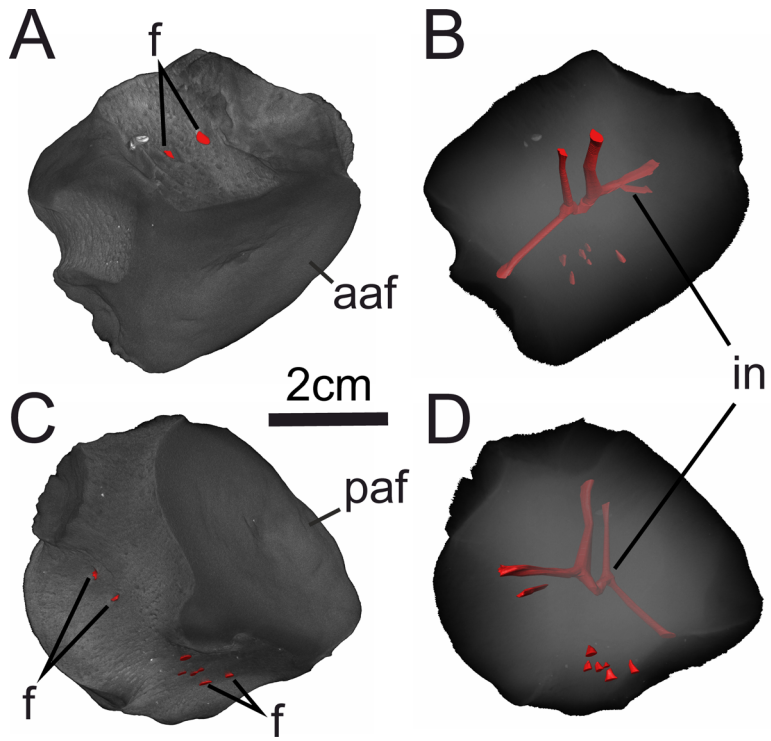

FIGURE 11. GG 422/3, CT renderings **A-D** of (caudal) vertebral centrum in **A, B** anterodorsolateral and **C, D** posteroventrolateral view. Abbreviations: aaf, anterior articular facet; f, foramen; in, internal network.

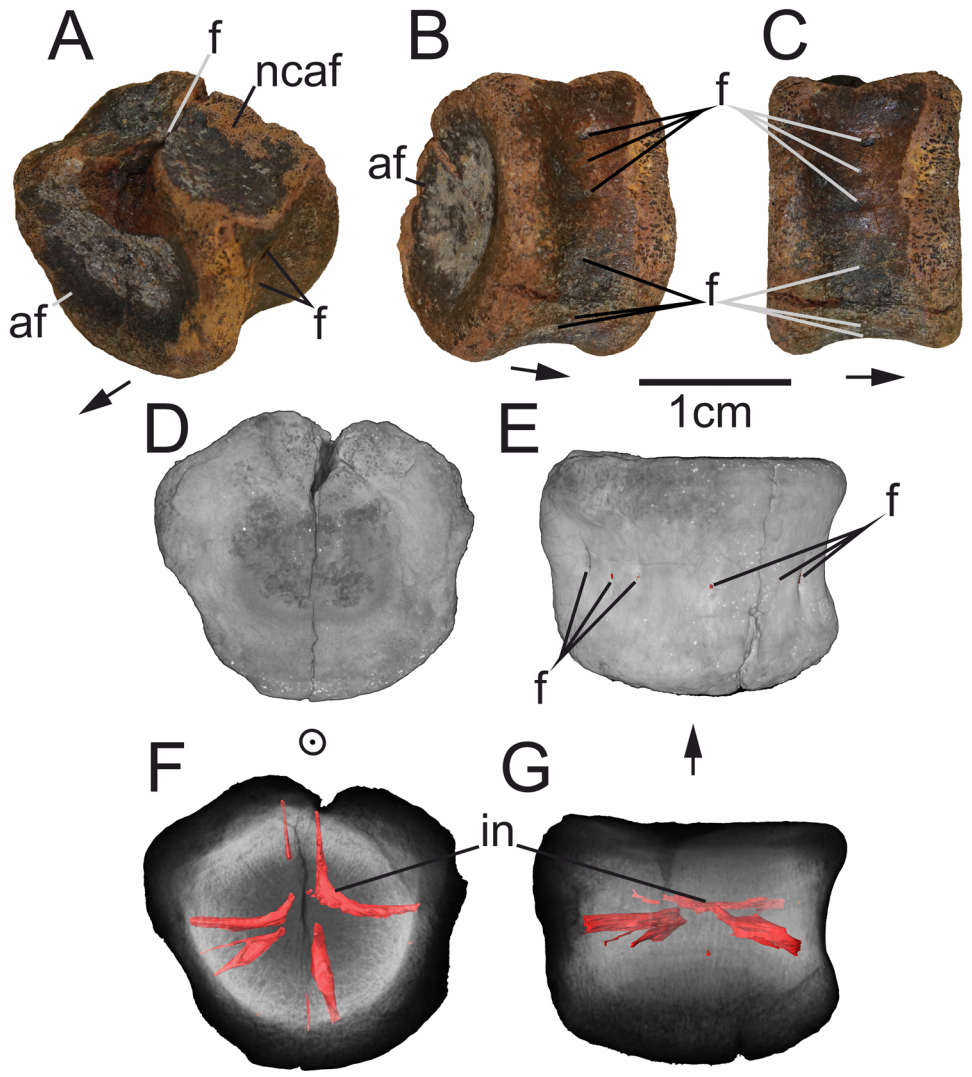

FIGURE 12. UHKD500005, photographs **A**, **B**, **C** of (?dorsal) vertebral centrum in **A** antero/posterodorsolateral, **B** antero/posteroventrolateral and **C** ventrolateral view. CT renderings **D**-**G** of UHKD500005 in **D**, **F** anterior/posterior view and **E**, **G** ventrolateral view. Abbreviations: af, articular facet; f, foramen; in, internal network; ncaf, neurocentral articular facet; tp, transverse process. Arrows point where the articular facet with the sediment cover faces.

The centra are approximately 3 cm in anteroposterior length and mediolateral width, and 2.5 cm in dorsoventral height. The anterior and posterior articular facets of the centra are subcircular in shape. The most complete transverse processes span around 7.5 cm mediolaterally, and the most complete neural spine is about 7.5 cm in dorsoventral height and 2.5 cm in anteroposterior width. The anteroposterior distance of the distalmost tips of the prezygapophyses to the respective postzygapophyses is around 3.5 cm. The centra seem slightly medially constricted. One of the centra clearly shows one ventrolateral foramen on each side around its mid-length (Figure 14C, D). The neurocentral sutures are still discernable in the vertebrae. The neural canals are drop-shaped, being dorsally tapered and ventrally rounded. The robust transverse processes are distally oval-shaped and dorsolaterally inclined. The articular facets of the prezygapophyses are slightly concave and face dorsomedially, while the articular facets of the postzygapophyses are slightly convex and face ventrolaterally. There are deep spinoprezygapophyseal and spinopostzygapophyseal fossae present on each vertrebra.

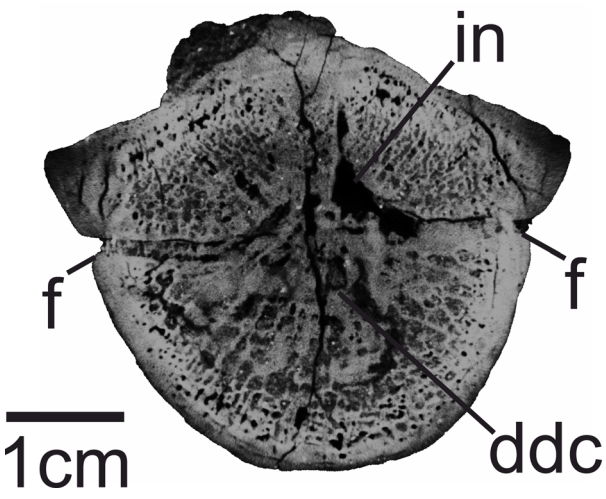

FIGURE 13. UHKD500005, CT image of mid-section. Abbreviations: ddc, distally diffuse cavity; f, foramen; in, internal network.

Provenance

The vertebrae of this study were found in (or were most likely in association with) Pleistocene deposits of northern Germany. The fossils were probably transported by the SIS from Mesozoic outcropping strata located in the southwestern Baltic Sea area. Especially clastic and calcareous Cretaceous rocks are dominating the near-surface pre-Quaternary lithologies in this region (Šliaupa and Hoth, 2011). Due to the existence of tectonic inversion structures around the island of Bornholm (Graversen, 2004; Svennevig and Surlyk, 2019), a widespread occurrence of Early to Late Cretaceous deposits are present and underlie the Quaternary strata.

As the specimen GG 501 was found as an isolated finding in a gravel pit of glacifluvial meltwater deposits with late-Weichselian age, a correlation to the post-Last Glacial Maximum advance of the SIS seems to be likely. The reconstructed ice advance direction of the corresponding glacier lobe occurred westward through the Baltic Sea basin (Hughes et al., 2016). Hereby, the area of Bornholm was overrun by the ice, and the specimen GG 501 was incorporated within the glacier bed, transported westwards and subsequently released during the final ice decay at the end of the Weichselian in northern Germany. The gravel pit in which the vertebra was found is located about 250 km west-southwest of Bornholm (Figure 1) and lies exactly in the stream direction of the former glacier movement (Hughes et al., 2016). Based on this, the source rock for specimen GG 501 most likely is located near or on the island of Bornholm.

Taxonomic Affinities and Axial Position

In respect to the diversity of secondarily aquatic tetrapods in the Mesozoic, a brief evaluation of the vertebrae in focus will be given. The previously undescribed vertebrae GG 501, GG 502 and UHKD500005 exhibit a greater similarity to plesiosaurs than to mosasaurs and ichthyosaurs. Mosasaurs typically have procoelous vertebrae (e.g., Street and Caldwell, 2017; Sachs et al., 2018), whereas ichthyosaurs have disk-like centra throughout the axial skeleton (e.g., McGowan and Motani, 2003; Maxwell et al., 2012), with a deep concavity on their anterior and posterior articular facets, distinct but simple neurocentral and lateral articular facets and no (large and obvious) foramina. Thus, all vertebrae can most likely be referred to as plesiosaurs (for GG 422/2, GG 422/3 and the unregistered GPIH vertebrae see Stumpf, 2016 and Sachs et al., 2016).

The vertebral column of plesiosaurs is organised into cervical, pectoral, dorsal, sacral and caudal vertebrae, which can be distinguished by the position of their rib facets (e.g., Brown, 1981; Sachs et al., 2013). Plesiosaur cervical vertebrae exhibit either a single or double-headed rib facet on either side of the centra. In contrast, pectorals differ in that the ribs articulate with a single facet that is positioned laterally on both the centrum and the neural arch. Dorsal centra have no parapophysis because ribs completely articulate with the elongated transverse process (Brown, 1981; Sachs et al., 2013). Caudal centra bear a single rib facet on either side of their centra and ventral haemal arch (chevron) facets (Brown, 1981; Sachs et al., 2016b).

Stumpf (2016) identified GG 422/2 (Figures 9, 10) as the cervical of an indetermined, osteologically mature (because of the closed neurocentral suture) plesiosauroid. The author suggested a posterior position within the neck because of the widely separated (larger and more laterally placed) ventral foramina (c. 2.5 cm apart) and because he considered the position of the rib facet to be on the mid-height of the centrum. However, only the dorsal-most margin of the rib facet reaches close to the mid-height of the centrum; instead, it is mostly situated in the ventral half. Because of the presence of ventral haemal arch facets in GG 422/3 (Figure 11), this specimen represents a caudal centrum of an indeterminate plesiosauroid, as originally identified by Stumpf (2016).

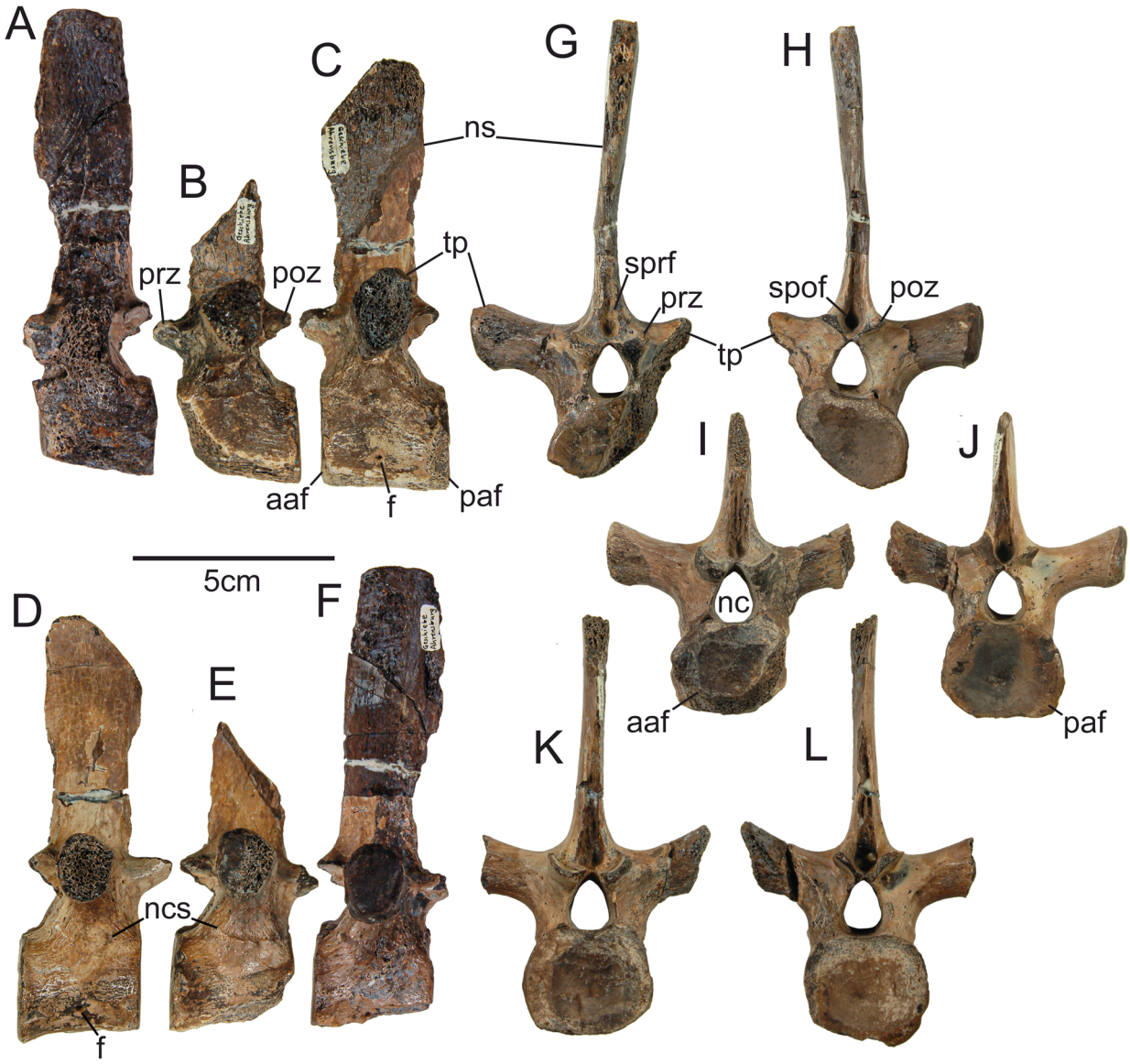

FIGURE 14. GPIH, unregistered, photographs of three dorsal vertebrae in **A**-**C** left lateral, **D**-**F** right lateral, **G**, **I**, **K** anterior and **H**, **J**, **L** posterior view. Abbreviations: aaf, anterior articular facet; f, foramen; nc, neural canal; ncs, neurocentral suture; ns, neural spine; paf, posterior articular facet; poz, postzygapophysis; prz, prezygapophysis; spof, spinopostzygaophyseal fossa; sprf, spinoprezygapophyseal fossa; tp, transverse process. Sachs et al. (2016a) show another order the individual vertebrae.

Under consideration of the height to length ratio (c. 1.4), as shown in Foth et al. (2011) and the prominent processes around the mid-height of the centrum, it may be that GG 501 (Figure 2) represents an anterior pectoral vertebra, possibly from an elasmosaurid or a polycotylid (see also Sachs et al., 2013). Nonetheless, GG 501 is remarkably wide mediolaterally, which may suggest a pliosaurid origin (see e.g., Vincent et al., 2013; however, the vertrebrae of long-necked plesiosaurs can be relatively wide as well, see Campbell et al., 2021). GG 502 (Figure 8) bears a remnant of the rib articulation process on the centrum, which may suggest a posterior pectoral position (see Sachs et al., 2013) and the vertebra falls inside the height and length ratios (1) of *Scanisaurus* Persson, 1959, elasmosaurids and polycotylids (Foth et al., 2011); the latter holds also true for the unregistered GPIH vertebrae (0.9; Figure 14). UHKD500005 (Figures 12, 13) does neither have a (transverse) process nor a parapophysis on the centrum (or haemal arch facets), which may suggest a dorsal position (see Sachs et al., 2016 a,b). However, UHKD500005 falls into the height/length ratio (1.4) of several ple-

siosaur groups (Foth et al., 2011) so that a more concrete taxonomic assignment is not possible.

Finally, Sachs et al. (2016) tentatively referred the unregistered GPIH dorsal vertebrae (Figure 14) to *Seeleyosaurus* White, 1940, which is accepted herein, although it is noteworthy that the dorsal centra of *Seeleyosaurus guilelmiimperatoris* (Dames, 1895) (MB.R 1992) from the late Early Jurassic Posidonienschiefer Formation of Holzmaden (southern Germany) tend to be stronger concave ventrally and the transverse processes seem rather posteriorly inclined. Furthermore, whereas Benson et al. (2012) suggested that a strong anteroposterior constriction on the base of dorsal neural spines is characteristic for *Microcleidus* Watson, 1909, we were unable to validate this (see e.g., Vincent et al., 2019), but rather see no or a modest constriction in the genus. This raises the assumption that the unregistered GPIH could also be referred to as *Microcleidus* due to a similar appearance.

Vertebral Vascularization Patterns During Ontogeny in Plesiosaurs

Following Araújo and Smith (2023), plesiosaur vertrebrae can be considered osteological immature with the neural arch and the centrum being unfused, whereas partially mature specimens still display a neurocentral suture. The fully mature stage is characterized by no externally visible neurocentral suture. In this sense, the most mature specimen examined here could be GG 422/2 (no visible neurocentral suture), followed by the osteological younger unregistered GPIH vertebrae (partly visible sutures) and the remaining specimens without a neural arch which could suggest incomplete fusion (however, these may also fell victim to erosion). However, fusion patterns in vertebrae of rhynchosaurs, phytosaurs and large-bodied non-avian theropods indicate that open neurocentral sutures on its own are not a reliable proxy for (im)maturity in reptiles, as the fusion can vary between different regions of the vertebral column within one individual, between different individuals of the same species and across different clades (Irmis, 2007; Heinrich et al., 2021; Griffin et al., 2021). Some secondary aquatic reptiles tend not to fuse their neurocentral sutures (skeletal paedomorphosis; Rieppel, 1989), but the situation has not been investigated for sauropterygians systematically.

Usually, the cervicals of plesiosaurs bear paired subcentral foramina (Romer, 1956), which are connected to a pair of foramina on the neural canal floor via simple, undivided internal canals (Wintrich et al., 2017). Hypothetically, these canals housed intersegmental arteries, representing vascular canals of vertebral precursors in early ontogenetic stages, which were later incorporated into the vertebrae (Wintrich et al., 2017). Hence, they do not represent blindly ending nutritive and oxygen supply for the respective bone, as is often the case in elements of the appendicular skeleton (Seymour et al., 2012). Unlike most other amniotes, plesiosaurs possibly retained these canals in their cervicals as paedomorphic osteological correlates (Wintrich et al., 2017). Wintrich et al. (2017) state that no subcentral or potential nutrient foramina were found in dorsal vertrebrae of plesiosaurs so far. However, Foth et al. (2011) mentioned dorsals of *Scanisaurus* with subcentral foramina, and at least one of the unregistered GPIH dorsal centra bears foramina on both sides ventrolaterally (also found in *Plesiosaurus dolichodeirus*, Vincent and Taquet, 2010; *Macroplata tenuiceps*, Ketchum and Smith, 2010; *Rhomaleosaurus thorntoni*, Smith and Benson, 2014). Thus, how do the internal canals found in our vertebrae, belonging to different regions within the vertebral column, fit into the mentioned narrative? According to Wintrich et al. (2017), canals that do not (blindly) end in or close to the core of the centrum (or center of ossification) are an argument against possible nutrient blood supply for a given vertebra. The transversal histological thin section of the posterior cervical SMNS 50845 from an undetermined plesiosaur of Holzmaden shows that the dorsal and ventral pairs of foramina are connected to a distally diffuse central cavity (Wintrich et al., 2017); a condition that is similarly developed in GG 422/3, GG 501, GG 502 and UHKD500005 (and possibly GG 422/2). Wintrich et al. (2017) state that their microCT data suggest separate internal canals that do not meet each other medially, and the apparent connection in SMNS 50845 can be explained by bone resorption or damage; however, our non-grinded vertebrae, suggesting internal connections, seem to preclude a damage. Furthermore, the symmetry (one pair of foramina dorsally and ventrally) is suggested to be typical for plesiosaur cervicals (Wintrich et al., 2017), which purportedly differs from the condition in whales which show dorsoventrally passing canals through the core of a vertebral centrum in an asymmetrical manner (Houssaye et al., 2015). We found asymmetrical conditions as well, which represents a known phenomenon in anatomy. The only internal feature that all vertebrae considered with microCT data herein have in common is the

presence of two main dorsal foramina and canals on the floor of the neural canal reaching close to the core of the respective centrum (Figures 2, 8-14). Three vertebrae have clear subcentral foramina (close to their anteroposterior mid-length) and deep-reaching canals on their ventral aspects (GG 422/2 [posterior cervical], GG 502 [posterior pectoral] and UHKD500005 [dorsal]). Deep canals and respective foramina on their ventrolateral aspects were found in GG 422/3 (caudal), GG 502, and UHKD500005 (and, potentially, GG 501 [anterior pectoral] but with a posterior deviation of the respective canals). At least one of the three unregistered GPIH vertebrae displays ventrolateral foramina as well. Additionally, GG 501 and UHKD500005 possess canals and respective foramina on their dorsal half (other than the ones on the neural canal floor). Furthermore, in GG 502, the internal network is not exactly situated in the anteroposterior mid-length of the centrum, which may weaken an intersegmental artery identity. Hence, no clear pattern of internal networks emerges, which may be due to phylogeny, ontogeny, individual expression, regionalization within the vertebral column, preservation and/or microCT data quality. Still, convincing evidence suggests the presence of complex vascular patterns within the vertebrae of plesiosaurs, which in turn indicates that these internal structures are not well-understood yet and need further investigation.

CONCLUSION

In the current study, we report on eight vertebrae of Mesozoic marine reptiles from different depositional and geographical contexts, five of which were examined with a microCT. Judging on a morphological basis, these isolated specimens likely belong to different axial positions of plesiosaurs, which were abundant dwellers of Mesozoic seas. A Mesozoic age, assumed for specimen GG 501, was confirmed by lithological and biostratigraphical investigations of the associated sediment. Thin section and calcareous nannofossil analyses revealed an early Cenomanian age of this specimen, which correlates to the base of the Arnager Greensand as an initial host rock. In addition, three long-known vertebrae (GPIH, unregistered) were depicted in more detail herein. Concluding, our microCT data facilitated the finding of novel (neuro)vascular patterns within plesiosaur vertebrae, which enriches the knowledge about the diversity of such patterns and possibly proves to be taxonomically, ontogenetically or position-related (within the vertebral column) relevant in the future. Furthermore, a multi-methodological approach (morphology, mineralogy, micropalaeontology) turns out to be useful to deal with isolated fossils such as erratics. Whereas CT examinations of dinosaur fossils, for example, are comparably widespread in the scientific literature, our knowledge about other fossil groups, such as plesiosaurs, could benefit from further expansion of such methods.

ACKNOWLEDGMENT

We thank G. Stollberg, J. Kopka, S. Ploetz and S. Polkowsky for their enthusiasm and kind cooperation. Thankfully, M. Hörnig scanned GG 502 and UHKD500005 (DFG INST 292/119-1 FUGG; DFG INST 292/120-1 FUGG), and S. Weinert produced thin the sections MV400005-TS and GG 501-TS. We also would like to thank M. Dockner (University of Vienna) for performing the scans of GG 422/2 and GG 501. U. Kotthoff (University of Hamburg) is acknowledged for providing access to the collection in his care. Furthermore, U. Stolpe, S. Meng, I. Hinz-Schallreuter, S. Harzsch, J. Kalbe, J. Ansorge, K. Obst and B. Englich supported this project. MK thanks the German Research Foundation (DFG) for financial support (KE 2023/2-1).

REFERENCES

Amalfitano, J., Giusberti, L., Fornaciari, E., Dalla Vecchia, F., Luciani, V., Kriwet, J., and Carnevale, G. 2019. Large deadfalls of the ‘ginsu’ shark *Cretoxyrhina mantelli* (Agassiz, 1835) (Neoselachii, Lamniformes) from the Upper Cretaceous of northeastern Italy. Cretaceous Research, 98:250–275 https://doi.org/10.1016/j.cretres.2019.02.003.

Araújo, R., and Smith, A. 2023. Recognising and quantifying the evolution of skeletal paedomorphosis in Plesiosauria. Fossil Record, 28:85–101. https://doi.org/10.3897/fr.26.97686

Bardet, N., Fischer, V., and Machalski, M. 2016. Large predatory marine reptiles from the Albian-Cenomanian of Annopol, Poland. Geological Magazine, 153:1–16. https://doi.org/10.1017/S0016756815000254.

Benson, R.B.J., Evans, M., and Druckenmiller, P. 2012. High diversity, low disparity and small body size in plesiosaurs (Reptilia, Sauropterygia) from the Triassic – Jurassic boundary. PLoS ONE, 7:e31838. https://doi.org/10.1371/journal.pone.0031838.

Bianucci, G., Bosio, G., Malinverno, E., de Muizon, C., Villa, I.M., Urbina, M., and Lambert, O. 2018. A new large squalodelphinid (Cetacea, Odontoceti) from Peru sheds light on the Early Miocene platanistoid disparity and ecology. Royal Society Open Science, 5:172302. https://doi.org/10.1098/rsos.172302.

Bown, P.R., Rutledge, D.C., Crux, J.A., and Gallagher, L.T. 1998. Lower Cretaceous. In Calcareous nannofossil biostratigraphy, In Bown, P. (ed.), 86–131. London: Chapman & Hall.

Bown, P.R. 2001. Calcareous nannofossils of the Gault, Upper Greensand and Glauconitic Marl (Middle Albian–Lower Cenomanian) from the BGS Selborne boreholes, Hampshire. Proceedings of the Geologists' Association, 112:223–236.

Brown, D.S. 1981. The English Upper Jurassic Plesiosauroidea (Reptilia) and a review of the phylogeny and classification of the Plesiosauria. Bulletin of the British Museum (Natural History), Geology Series, 35:253–347.Burnett, J.A. 1998. Upper Cretaceous. In Calcareous nannofossil biostratigraphy, In Bown, P. (ed.), 132–199. London: Chapman & Hall.

Campbell, J.A., Mitchell, M.T., Ryan, M.J., and Anderson, J.S. 2021. A new elasmosaurid (Sauropterygia: Plesiosauria) from the non-marine to paralic Dinosaur Park Formation of southern Alberta, Canada. PeerJ, 9:e10720. https://doi.org/10.7717/peerj.10720

Christensen, W.K. and Schulz, M.-G. 1997. Coniacian and Santonian belemnite faunas from Bornholm, Denmark. Fossils and Strata, 44:1–77.

Cohen, K.M., Finney, S.C., Gibbard, P.L., and Fan, J.-X. 2013 (updated). The ICS International Chronostratigraphic Chart. Episodes 36:199–204. http://www.stratigraphy.org/ICSchart/ChronostratChart2021-10.pdf

Dames, W. 1895. Die Plesiosaurier der Süddeutschen Liasformation. Abhandlungen der Königlich Preussischen Akademie der Wissenschaften zu Berlin, 2:1–83.

De Blainville, H.-M.D. 1835. Description de quelques espèces de reptiles de la Californie: précédée de l'analyse d'un systéme général d'Erpétologie et d'Amphibiologie Nouvelles Annales du Muséum d'Historie Naturelle, Paris, Reptiles de la Californie, 4:233–296.

De Keyser, T.L. 1999. Digital scanning of thin sections and peels. Journal of Sedimentary Research 69:962–964. https://doi.org/10.2110/jsr.69.962

Fischer, V., Benson, R.B.J., Zverkov, N.G., Soul, L.C., Arkhangelsky, M.S., Lambert, O., Stenshin, I.M., Uspensky, G.N., and Druckenmiller, P.S. 2017. Plasticity and convergence in the evolution of short-necked plesiosaurs, Current Biology, 27:1667–1676.e3. https://doi.org/10.1016/j.cub.2017.04.052

Foth, C., Kalbe, J., and Kautz, J. 2011. First evidence of Elasmosauridae (Reptilia: Sauropterygia) in an erratic boulder of Campanian age originating from southern Sweden or the adjacent Baltic Sea area. Zitteliana, A51:285–290.

Graversen, O. 2004. Upper Triassic – Cretaceous stratigraphy and structural inversion off-shore SW Bornholm, Tornquist Zone, Denmark. Bulletin of the Geological Society of Denmark, 51:111–136.

Griffin, C.T., Stocker, M.R., Colleary, C., Stefanic, C.M., Lessner, E.J., Riegler, M., Formoso, K.K., Koeller, K., and Nesbitt, S.J. 2021. Assessing ontogenetic maturity in extinct saurian reptiles. Biological Reviews, 96:470–525.

Hajny, C. 2016. Sedimentological study of the Jurassic and Cretaceous sequence in the Revinge-1 core, Scania. PhD thesis, Lund University. https://lup.lub.lu.se/student-papers/record/8871238/file/8871241.pdf Accessed 08 November 2021.

Hart, M.B. 1979. Biostratigraphy and palaeozoogeography of planktonic Foraminiferida from the Cenomanian of Bornholm, Denmark. Newsletters in Stratigraphy, 8:83–96. https://doi.org/10.1127/nos/8/1979/83

Hart, M.B., Bromley, R.G., and Packer, S.R. 2012. Anatomy of the stratigraphical boundary between the Arnager Greensand and Arnager Limestone (Upper Cretaceous) on Bornholm, Denmark. Proceedings of the Geologists' Association, 123:471–478. https://doi.org/10.1016/j.pgeola.2011.11.006

Heinrich, C., Paes Neto, V.D., Lacerda, M.B., Martinelli, A.G., Fiedler, M.S., and Schultz, C.L. 2021. The ontogenetic pattern of neurocentral suture closure in the axial skeleton of Hyperodapedontine (Archosauromorpha, Rhynchosauria) and its evolutionary implications. Palaeontology, 64:409–427.

Houssaye, A., Tafforeau, P., de Muizon, C., and Gingerich P.D. 2015. Transition of Eocene whales from land to sea: evidence from bone microstructure. PLoS ONE, 10(2):e0118409. https://doi.org/10.1371/journal.pone.0118409

Hughes, A., Gyllencreutz, R., Lohne, Ø., Mangerud, J., and Svendsen, J. 2015. The last Eurasian ice sheets – a chronological database and time-slice reconstruction, DATED-1. Boreas, 45. https://doi.org/10.1111/bor.12142

Irmis, R.B. 2007. Axial skeleton ontogeny in the Parasuchia (Archosauria: Pseudosuchia) and its implications for ontogenetic determination in archosaurs. Journal of Vertebrate Paleontology, 27:350–361.

Lehmann, U. 1971. Faziesanalyse der Ahrensburger Liasknollen auf Grund ihrer Wirbeltierreste. Mitteilungen aus dem Geologischen Institut der Technischen Universität Hannover, 10:21–42.

Lierl, H.-J. 1993. Exkursionsführer zur Geologie des Kreises Herzogtum Lauenburg. Geschiebekunde aktuell, Sonderheft, 3:1–36.

Landesamt für Umwelt, Naturschutz und Geologie (LUNG) Mecklenburg-Vorpommern (2010): Geologische Karte von Mecklenburg-Vorpomern – Übersichtskrate 1:500 000 - An der Oberfläche und am angrenzenden Ostseegrund auftretenden Bildungen. Güstrow.

Ketchum, H.F. and Smith, A.S. 2010. The anatomy and taxonomy of *Macroplata tenuiceps* (Sauropterygia, Plesiosauria) from the Hettangian (Lower Jurassic) of Warwickshire, United Kingdom. Journal of Vertebrate Paleontology, 30(4):1069-1081. https://doi.org/10.1080/02724634.2010.483604

MacKenzie, W.S., Adams, A.E., and Brodie, K. 2017. Rocks and Minerals in Thin Section. Leiden: CRC Press/Balkema.

Madzia, D. 2016. A reappraisal of *Polyptychodon* (Plesiosauria) from the Cretaceous of England. PeerJ, 4:e1998. https://doi.org/10.7717/peerj.1998

McGowan, C. and Motani, R. 2003. Handbook of Paleoherpetology. Part 8: Ichthyopterygia. Verlag Dr. Friedrich Pfeil.

Maxwell, E.E., Fernández, M.S., and Schoch, R.R. 2012. First diagnostic marine reptile remains from the Aalenian (Middle Jurassic): a new ichthyosaur from southwestern Germany. PLoS One, 7, e41692.

Owen, R. 1860. On the orders of fossil and recent Reptilia, and their distribution in time. Reports of the British Association for the Advancement of Science, London, 29:153–166.

Perch-Nielsen, K. 1985. Mesozoic calcareous nannofossils. In Plankton Stratigraphy, vol. 1, Bolli, H.M., Saunders, J.B., and Perch-Nielsen, K. (eds.), 329–426. Cambridge: Cambridge University Press.

Persson, P.O. 1959. Reptiles from the Senonian (U. Cret.) of Scania (S. Sweden). Arkiv för Mineralogi och Geologi, 2:431–478.

Persson, P.O. 1963. A revision of the classification of the Plesiosauria with a synopsis of the stratigraphical and geographical distribution of the group. Lunds Universitets Ãrsskrift, N.F. Avdelningen 2, 1e59.

Rieppel, O.C. 1989. *Helveticosaurus zollingeri* Peyer (Reptilia, Diapsida) skeletal paedomorphosis, functional anatomy and systematic affinities. Palaeontographica, Abt. A 208:123–152.

Romer, A.S. 1956. *Osteology of the Reptiles*, The University of Chicago Press, Chicago, 772 pp.

Sachs S., Kear, B.P., and Everhart, M.J. 2013. Revised vertebral count in the "longest-necked vertebrate" *Elasmosaurus platyurus* Cope 1868, and clarification of the cervical-dorsal transition in Plesiosauria. PLoS ONE, 8(8):e70877. https://doi.org/10.1371/journal.pone.0070877

Sachs, S., Hornung, J., Liehrl, H.-J., and Kear, B.P. 2016a. Plesiosaurian fossils from Baltic glacial erratics: evidence of Early Jurassic marine amniotes from the southwestern margin of Fennoscandia. In Kear, B.P., Lindgren, J., Hurum, J.H., Mílan, J., and Vajada, V. (eds.), Mesozoic Biotas of Scandinavia and its Arctic Territories. – Geological Society, London, Special Publications, 434.
https://doi.org/10.1144/SP434.14

Sachs, S., Hornung, J.J., and Kear, B.P. 2016b. Reappraisal of Europe's most complete Early Cretaceous plesiosaurian: *Brancasaurus brancai* Wegner, 1914 from the ''Wealden facies'' of Germany. PeerJ, 4, e2813.
https://doi.org/10.7717/peerj.2813

Sachs, S., Hornung, J.J., and Scheer, U. 2018. Mosasaurid and plesiosaurian remains from marginal facies of the lower Campanian (Upper Cretaceous) Bottrop and Vaals formations of western Germany. Cretaceous Research, 87:358–367.
https://doi.org/10.1016/j.cretres.2017.05.026

Schade, M. and Ansorge, J. 2022. New thyreophoran dinosaur material from the Early Jurassic of northeastern Germany. PalZ, 96:303–311.
https://doi.org/10.1007/s12542-022-00605-x

Schiøler, P. 1992. Dinoflagellate cysts from the Arnager Limestone Formation (Coniacian, Late Cretaceous), Bornholm, Denmark. Review of Palaeobotany and Palynology, 72:1–125.

Seymour, R.S., Smith, S.L., White, C.R., Henderson, D.M., and Schwarz-Wings, D. 2012. Blood flow to long bones indicates activity metabolism in mammals, reptiles and dinosaurs. Proceedings of the Royal Society B, 279:451–456.

Shogenova, A., Fabricius, I.L., Korsbech, U., Rasteniene, V., and Sliaupa, S. 2003 Glauconitic rocks in the Baltic area: estimation of specific surface. Proceedings of the Estonian Academy of Sciences. Geology, 52:69–86.

Šliaupa, S. and Hoth, P. 2011. Geological Evolution and Resources of the Baltic Sea Area from the Precambrian to the Quaternary. In Harff, J., Björck, S., and Hoth, P. (eds.) The Baltic Sea Basin – Central and Eastern European Development Studies (CEEDES), Berlin, 13–51.

Smith, A.S., and R.B.J. Benson. 2014. Osteology of *Rhomaleosaurus thorntoni* (Sauropterygia: Rhomaleosauridae) from the Lower Jurassic (Toarcian) of Northamptonshire, England. Monographs of the Palaeontographical Society, 168(642):1–40.
https://doi.org/10.1080/02693445.2014.11963953

Street, H., and M. Caldwell. 2017. Rediagnosis and redescription of *Mosasaurus hoffmannii* (Squamata: Mosasauridae) and an assessment of species assigned to the genus *Mosasaurus*. Geological Magazine, 1:1–37.
https://doi.org/10.1017/S0016756816000236

Stumpf, S. 2016. New information on the marine reptile fauna from the lower Toarcian (Early Jurassic) "Green Series" of North-Eastern Germany. Neues Jahrbuch für Geologie und Paläontologie, Abhandlungen, 280(1):87–105.

Stumpf, S., and J. Kriwet. 2019. A new Pliensbachian elasmobranch (Vertebrata, Chondrichthyes) assemblage from Europe, and its contribution to the understanding of late Early Jurassic elasmobranch diversity and distributional patterns. PalZ, 93:637–658.
https://doi.org/10.1007/s12542-019-00451-4

Svennevig, K., and F. Surlyk. 2019. A high-stress shelly fauna associated with sponge mud-mounds in the Coniacian Arnager Limestone of Bornholm, Denmark. Lethaia, 52:57–76.
https://doi.org/10.1111/let.12290

Watkins, D.K., and J.A. Bergen. 2003. Late Albian adaptive radiation in the calcareous nannofossil genus *Eiffellithus*. Micropaleontology, 49(3):231–252.

Watson, D.M.S. 1909. IV. A preliminary note on two new genera of upper Liassic plesiosaurs. Memoirs and Proceedings of the Manchester Literary and Philosophical Society, 54:1–28.

Welles, S.P. 1943. Elasmosaurid plesiosaurs with a description of new material from California and Colorado. University of California, Publications in Geological Sciences, 13:125–215.

White, T.E. 1940. Holotype of *Plesiosaurus longirostris* Blake and the classification of the plesiosaurs. Journal of Paleontology, 14:451–467.

Williams-Mitchell, E. 1948. The zonal value of foraminifera in the Chalk of England. Proceedings of the Geologists' Association, 59:96–112.

Wintrich, T., M. Scaal, and P.M. Sander. 2017. Foramina in plesiosaur cervical centra indicate a specialized vascular system. Fossil Record, 20:279–290.
https://doi.org/10.5194/fr-20-279-2017

Wintrich T., S. Hayashi, A. Houssaye, Y. Nakajima, and M. Sander. 2017. A Triassic plesiosaurian skeleton and bone histology inform on evolution of a unique body plan. Science Advances, 3:e1701144. https://doi.org/10.1126/sciadv.1701144

Vincent, P., and P. Taquet. 2010. A plesiosaur specimen from the Lias of Lyme Regis: The second ever discovered plesiosaur by Mary Anning. Geodiversitas, 32.

Vincent, P., N. Bardet, and E. Mattioli. 2013. A new pliosaurid from the Pliensbachian (Early Jurassic) of Normandy (Northern France). Acta Palaeontologica Polonica, 58(3):471–485.

Vincent, P., R. Weis, G. Kronz, and D. Delsate. 2019. *Microcleidus melusinae*, a new plesiosaurian (Reptilia, Plesiosauria) from the Toarcian of Luxembourg. Geological Magazine, 156(1):99–116. https://doi.org/10.1017/S0016756817000814

TAXONOMIC INDEX OF CALCAREOUS NANNOFOSSILS

Axopodorhabdus albianus (Black, 1967) Wind & Wise, *in* Wise & Wind, 1977

Biscutum constans (Górka, 1957) Black *in* Black & Barnes, 1959

Broinsonia matalosa (Stover, 1966) Burnett *in* Gale et al., 1996

Broinsonia signata (Noël, 1969) Noël, 1970

Bukrylithus ambiguus Black, 1971

Calciosolenia fossilis (Deflandre *in* Deflandre & Fert, 1954) Bown *in* Kennedy et al., 2000

Chiastozygus litterarius (Górka, 1957) Manivit, 1971

Chiastozygus platyrhethus Hill, 1976

Chiastozygus spissus Bergen *in* Bralower & Bergen, 1998

Chiastozygus synquadriperforatus Bukry, 1969

Cribrosphaerella ehrenbergii (Arkhangelsky, 1912) Deflandre *in* Piveteau, 1952

Cyclagelosphaera margerelii Noël, 1965

Discorhabdus ignotus (Górka, 1957) Perch-Nielsen, 1968

Eiffellithus equibiramus Watkins & Bergen, 2003

Eiffellithus monechiae Crux, 1991

Eiffellithus paragogus Gartner *in* Robaszynski et al., 1993

Eiffellithus turriseiffelii (Deflandre *in* Deflandre & Fert, 1954) Reinhardt, 1965

Eprolithus apertior Black, 1973

Gartnerago theta (Black *in* Black & Barnes, 1959) Jakubowski, 1986

Gorkaea operio Varol & Girgis, 1994

Helicolithus compactus (Bukry, 1969) Varol & Girgis, 1994

Lithraphidites acutus subsp. *acutus* Verbeek & Manivit *in* Manivit et al., 1977

Manivitella pemmatoidea (Deflandre *in* Manivit, 1965) Thierstein, 1971

Prediscosphaera columnata (Stover, 1966) Perch-Nielsen, 1984

Prediscosphaera cretacea (Arkhangelsky, 1912) Gartner, 1968

Radiolithus orbiculatus (Forchheimer, 1972) Varol, 1992

Radiolithus planus Stover, 1966

Radiolithus undosus (Black, 1973) Varol, 1992

Repagulum parvidentatum (Deflandre & Fert, 1954) Forchheimer, 1972

Retecapsa crenulata (Bramlette & Martini, 1964) Grün *in* Grün & Allemann, 1975

Rhagodiscus angustus (Stradner, 1963) Reinhardt, 1971

Rhagodiscus hamptonii Bown *in* Kennedy et al., 2000

Rhagodiscus splendens (Deflandre, 1953) Verbeek 1977

Rotelapillus crenulatus (Stover, 1966) Perch-Nielsen, 1984

Sollasites horticus (Stradner et al. *in* Stradner & Adamiker, 1966) Cepek & Hay, 1969

Staurolithites ellipticus (Gartner, 1968) Lambert, 1987

Staurolithites gausorhethium (Hill, 1976) Varol & Girgis, 1994

Staurolithites laffittei Caratini, 1963

Tegumentum stradneri Thierstein *in* Roth & Thierstein, 1972

Tranolithus orionatus (Reinhardt, 1966a) Reinhardt, 1966b

Tubodiscus burnettiae Bown *in* Kennedy et al., 2000

Watznaueria barnesiae (Black *in* Black & Barnes, 1959) Perch-Nielsen, 1968

Watznaueria baticlypeata (Bukry, 1969) comb. nov. cf. Young et al., 2018

Zeugrhabdotus acanthus Reinhardt, 1965

Zeugrhabdotus bicrescenticus (Stover, 1966) Burnett *in* Gale et al., 1996

Zeugrhabdotus diplogrammus (Deflandre *in* Deflandre & Fert, 1954) Burnett *in* Gale et al., 1996

Zeugrhabdotus embergeri (Noël, 1959) Perch-Nielsen, 1984

Zeugrhabdotus erectus (Deflandre *in* Deflandre & Fert, 1954) Reinhardt, 1965

Zeugrhabdotus howei Bown *in* Kennedy et al., 2000

Zeugrhabdotus trivectis Bergen, 1994

Zeugrhabdotus xenotus (Stover, 1966) Burnett, *in* Gale et al., 1996